Copy
RM L50J20

NACA RM L50J20

NACA

RESEARCH MEMORANDUM

LOW-SPEED INVESTIGATION OF THE EFFECT OF SEVERAL FLAP AND SPOILER AILERONS ON THE LATERAL CHARACTERISTICS OF A 47.5° SWEPTBACK-WING - FUSELAGE COMBINATION AT A REYNOLDS NUMBER OF 4.4×10^6

By Jerome Pasamanick and Thomas B. Sellers

Langley Aeronautical Laboratory
Langley Air Force Base, Va.

NATIONAL ADVISORY COMMITTEE
FOR AERONAUTICS

WASHINGTON

December 8, 1950

NACA RM L50J20

NATIONAL ADVISORY COMMITTEE FOR AERONAUTICS

RESEARCH MEMORANDUM

LOW-SPEED INVESTIGATION OF THE EFFECT OF SEVERAL FLAP AND SPOILER AILERONS ON THE LATERAL CHARACTERISTICS OF A 47.5° SWEPTBACK-WING - FUSELAGE COMBINATION AT A REYNOLDS NUMBER OF 4.4×10^6

By Jerome Pasamanick and Thomas B. Sellers

SUMMARY

An investigation was made in the Langley full-scale tunnel of the low-speed lateral characteristics of a 47.5° sweptback-wing - fuselage combination with several flap and spoiler aileron arrangements at a Reynolds number of 4.4×10^6. The wing had an aspect ratio of 3.4, a taper ratio of 0.51, and NACA 64_1A112 airfoil sections. The results indicated that the rolling effectiveness of small-span ailerons located inboard of the wing tips were greater than the effectiveness of equal-span ailerons located at the wing tips. At lift coefficients near the stall, the aileron effectiveness of the model with thick trailing-edge contour ailerons was essentially the same as the aileron effectiveness of the original contour ailerons.

In general, the spoilers located in the region of the plane of symmetry developed greater rolling moments than equal-span spoilers located at the wing tip. Increasing spoiler projection increased the spoiler rolling moments and spoiler chordwise location had no appreciable effects on the rolling moments of the model at the angle of attack corresponding to 85 percent of the maximum lift.

INTRODUCTION

Lateral-control devices designed for airplanes flying at high speeds may produce unsatisfactory lateral characteristics at the lower flight speeds. Much research has been made to investigate the lateral characteristics of swept and unswept wings and low-aspect-ratio and high-aspect-ratio wings equipped with several types of lateral-control devices

(references 1 to 4 and unpublished results). In order to supplement further the data of the above references, an investigation has been made at a high Reynolds number in the Langley full-scale tunnel on a 47.5° sweptback wing having an aspect ratio of 3.4 and a taper ratio of 0.51.

The data presented herein include test results of a 19-percent-chord plain-flap aileron having various spans and trailing-edge thicknesses. The effects of spoiler spanwise and chordwise location and projection on the lateral characteristics of the model are also shown. The results are presented for the basic wing and the wing with extensible leading-edge and plain trailing-edge flaps through a range of angles of attack from small negative angles through maximum lift at a Reynolds number of approximately 4.4×10^6 and a Mach number of 0.07.

SYMBOLS

The data are presented with respect to the wind axes originating in the plane of symmetry at the quarter-chord point of the mean aerodynamic chord. The X-axis is in the plane of symmetry and parallel to the tunnel air flow. The Z-axis is in the plane of symmetry and perpendicular to the X-axis, and the Y-axis is perpendicular to the plane of symmetry. All forces and moments are referred to the quarter chord of the mean aerodynamic chord.

C_L	lift coefficient (Lift/qS)
C_D	drag coefficient (Drag/qS)
C_m	pitching-moment coefficient (Pitching moment/qS$\bar{c}$)
C_l	rolling-moment coefficient (Rolling moment/qSb)
C_n	yawing-moment coefficient (Yawing moment/qSb)
S	total wing area, square feet
b	wing span measured normal to plane of symmetry, feet
c	wing chord, measured in plane perpendicular to quarter-chord line, feet
c'	wing chord measured in plane parallel to plane of symmetry, feet

[redacted]

$\bar{c}$ wing mean aerodynamic chord measured in plane parallel to plane of symmetry, feet $\left(\frac{2}{S}\int_0^{b/2} c'^2 dy\right)$

y lateral distance from plane of symmetry along Y-axis, feet

q free-stream dynamic pressure, pounds per square foot $\left(\frac{1}{2}\rho V^2\right)$

ρ mass density of air, slugs per cubic foot

V free-stream velocity, feet per second

b_f flap span measured normal to plane of symmetry, feet

b_a aileron span measured normal to plane of symmetry, feet

b_s spoiler span measured normal to plane of symmetry, feet

δ_a aileron deflection measured normal to aileron hinge line, positive when trailing edge is deflected downward, degrees

δ_s spoiler projection, measured normal to wing surface in a plane parallel to plane of symmetry, fraction chord

t aileron trailing-edge thickness, measured in a plane perpendicular to aileron hinge axis, fraction of aileron-hinge-axis thickness

α angle of attack of wing chord line, measured in plane of symmetry, degrees

Δ increment of coefficient due to aileron deflection or spoiler projection

$C_{l_{\delta_a}} = \frac{\partial C_l}{\partial \delta_a}$, per degree

Subscripts:

o outboard

a aileron

s spoiler

[redacted]

T total aileron deflection

LE extensible leading-edge flaps

TE plain trailing-edge flaps

MODEL

The general dimensions of the wing-fuselage combination are given in the three-view drawing of figure 1 and a photograph of the model mounted in the Langley full-scale tunnel is presented in figure 2. The wing leading-edge sweepback was 47.5°, the aspect ratio was 3.4, the taper ratio was 0.51, and the airfoil sections normal to the quarter-chord line were NACA 64_1A112. The wing was constructed without dihedral or twist and was mounted in a low midwing position at zero incidence on a circular fuselage.

The flap configurations tested in conjunction with the lateral-control devices were determined from the results given in reference 5 and consisted of extensible leading-edge and plain trailing-edge flaps. Details of the flaps are given in figure 3(a). The extensible leading-edge flaps were 0.10c' and extended over the outboard 35 percent of each wing semispan. The angle of deflection of the leading-edge flaps when not used in conjunction with the trailing-edge flaps was 150° and when combined with the trailing-edge flaps was 135° (measured in a plane parallel to the plane of symmetry). The plain trailing-edge flaps used in this investigation had a chord of 0.19c and extended outboard from the 12-percent-semispan station to the 55-percent-semispan and 77.5-percent-semispan stations. The flaps deflected 40° from the chord plane normal to the hinge line.

The lateral-control devices employed in the present investigation were plain flap ailerons and plain upper-surface spoilers as shown in figure 3(b). The ailerons were 0.19c and spanned the outboard 22.5 percent and 45 percent of the wing semispan. For all aileron tests, the right-wing aileron was deflected down and the left-wing aileron was equally deflected in the opposite direction. The aileron-deflection-angle range varied from the neutral position to 28° at 4° increments measured normal to the hinge line. In addition to the original contour ailerons, straight-sided covers were fitted over the ailerons tangent to the surface at the hinge line and formed trailing-edge thicknesses of 25 percent, 50 percent, and 75 percent of the aileron hinge-line thickness. The included aileron trailing-edge angle was reduced from 14.2° for the basic contour to approximately 10.4°, 6.7°, and 3.7° for the respective aileron trailing-edge thicknesses.

[redacted]

The spoilers were mounted on the left wing perpendicular to the wing upper surface and were constructed in four sections between the 12-percent-semispan and 97.5-percent-semispan stations. The spoilers were located on the 0.70c line and the span was varied by fixing the spoiler at either end (root or tip) and successively adding sections until the maximum spoiler span was attained. The spoiler heights investigated included projections of 2 percent, 5 percent, and 10 percent of the wing chord measured in a plane parallel to the plane of symmetry. A 0.10c' partial-span spoiler configuration $\left(b_s = 0.63\frac{b}{2},\ y_{s_0} = 0.86\frac{b}{2}\right)$ was investigated at the 50-percent and at the 70-percent chordwise stations. The effect of spoiler shape was also determined for this configuration. The spoiler was perforated with 1-inch-diameter holes located 2 inches on center in staggered rows; thus, 17.8 percent of the spoiler area was removed.

TESTS

The tests were made on the six-component balance system of the Langley full-scale tunnel at a Reynolds number of 4.4×10^6 and a Mach number of approximately 0.07. Data were obtained at zero yaw over a range of angles of attack from small negative angles through maximum lift.

RESULTS

All the data have been corrected for blocking effects, stream alinement, and approximate wing-support interference. The drag and angle-of-attack data have been corrected for jet-boundary effects (as determined from the straight-wing method of reference 6) but although the corrections for the effects of the jet boundary on the moment data have not been applied they are considered negligible. The aileron-effectiveness parameter $C_{l_{\delta_a}}$ was obtained by measuring the slopes of rolling-moment curves from 0° to 20° total aileron deflection for several values of angle of attack below the maximum lift. All wing configurations, without ailerons or spoilers, exhibited small values of rolling-moment and yawing-moment coefficients as a result of the slight irregularities of the model construction, model test mounting, and tunnel air flow. The data reported herein have not been corrected for the initial out-of-trim roll or yaw of the model when the controls were neutral.

In order to facilitate the discussion of results, the data are arranged in the following order of figures. Figure 4 presents the static

longitudinal characteristics of the model with and without flaps as obtained from reference 5. The effects of aileron span and trailing-edge thickness on the aileron-effectiveness parameter are presented in the summary curves of figures 5 and 6 for the wing with and without flaps. Figure 7 shows the effects of spoiler span on the rolling characteristics of the plain- and flapped-wing configurations, and figure 8 presents a comparison between the estimated and measured rolling coefficients of the model with a partial-span spoiler. The rolling characteristics of a full-span spoiler with various projection heights are given in figure 9 over a range of angles of attack. The effects of spoiler chordwise location on the lateral characteristics of the model having a partial-span spoiler are given in figure 10. Figure 11 compares the lateral characteristics of the model equipped with several ailerons and spoilers. The basic aerodynamic characteristics of the model having ailerons of various spans, spanwise locations, and trailing-edge thicknesses are given in figures 12 to 15, and the basic spoiler data are presented in figures 16 to 18 for the plain- and flapped-wing configurations. Figure 19 presents the effects of a perforated partial-span spoiler on the aerodynamic characteristics of the model.

DISCUSSION OF RESULTS

Aileron Control Characteristics

Effect of aileron span and spanwise location.- As might be expected, the results given in figure 5 show that the aileron-effectiveness parameter $C_{l_{\delta_a}}$ increased with aileron span with the greatest value of $C_{l_{\delta_a}}$ being obtained at the lowest angle of attack. The aileron effectiveness at the angle of attack corresponding to 85 percent of the maximum lift coefficient, which shall be referred to throughout the discussion inasmuch as it is usually considered the highest landing approach lift coefficient, was approximately 75 percent of the maximum value of $C_{l_{\delta_a}}$ obtained for each wing configuration. For the plain wing at $0.85C_{L_{max}}$, the aileron effectiveness of equal-span ailerons $\left(0.225\frac{b}{2}\right)$ located at the wing tip or inboard of the $0.775\frac{b}{2}$-span station was -0.00024 or -0.00030, respectively. Tuft observations indicated the flow over the rear and outboard sections of the wing to be unsteady with the effect being more pronounced near the wing tip. Increasing the aileron span to $0.45\frac{b}{2}$ (outboard end located at the wing tips) resulted in a value of $C_{l_{\delta_a}}$ of -0.00054. This value is more than double the value of $C_{l_{\delta_a}}$ obtained

[redacted]

from the $0.225\frac{b}{2}$ - span aileron located at the wing tip. The increment of aileron effectiveness produced by each equal-span aileron $\left(0.225\frac{b}{2}\right)$ at the spanwise locations investigated can be added to produce a total $C_{l_{\delta_a}}$ for the $0.45\frac{b}{2}$ - span aileron at $0.85C_{L_{max}}$. At lower angles of attack, however, this procedure slightly overestimates the effectiveness of the $0.45\frac{b}{2}$ - span ailerons. The aileron effectiveness (-0.00051) at $0.85C_{L_{max}}$ of the $0.45\frac{b}{2}$ - span ailerons located on the flapped-wing configurations were essentially the same as the results for the plain wing.

The results given in figures 12 to 14 show the variation of rolling-moment and yawing-moment coefficients to be linear with total aileron deflection for the model configurations tested. In general, aileron deflection produced adverse yaw for all wing configurations with the effect becoming more adverse with increasing lift coefficient and aileron deflection. The lift and pitching-moment characteristics were essentially unaffected by the deflection of the ailerons and the increment of drag coefficient (fig. 15) was small compared to the total model drag at a lift coefficient of approximately $0.85C_{L_{max}}$.

Effect of aileron trailing-edge thickness.- The results given in references 7 and 8 show that improvements in the rolling characteristics at both high and low flight speeds of sweptback wings can be obtained with ailerons having finite trailing-edge thickness. Reference 3 indicates that decreasing the aileron trailing-edge angle would also improve the rolling characteristics of the configuration. The results of figure 6 show that in the lift range of approximately $0.85C_{L_{max}}$ there is some increase in $C_{l_{\delta_a}}$ for the 0.25t small-span ailerons located at the wing tip on the basic wing configuration, but for thicknesses greater than 0.25t there is no appreciable effect or a slight loss in effectiveness. With leading-edge flaps deflected, the finite trailing-edge thick ailerons had negligible effects on the aileron effectiveness in the high-lift range. From low-speed considerations, it appears that a thick trailing-edge aileron would give about the same rolling effectiveness as the original contour aileron. At this lift coefficient $\left(0.85C_{L_{max}}\right)$ tuft observations indicated that the ailerons are operating in regions of unsteady and stalled flow and the thick trailing-edge ailerons did not noticeably influence the flow characteristics ahead of the aileron hinge line. The drag increments for all model configurations (fig. 15) near the stall, as a result of the thick ailerons, were small for all model configurations and for some conditions the thick ailerons resulted in drag decrements. The lift and pitching-moment coefficients (figs. 12 and 13) were essentially unaffected by the addition of the finite thickness ailerons and were generally constant with aileron deflection angle.

[redacted]

Spoiler-Control Characteristics

Effect of spoiler-span and spanwise location.- The rolling-moment coefficient of the model as shown in figure 7 increased with spoiled span and the angles of attack for maximum spoiler effectiveness were approximately 6.9° for the basic wing configuration and 12° for the flapped-wing configuration. Tuft observations showed the flow over the outboard sections to be disturbed and a pronounced spanwise flow of the boundary layer occurred along the rearward portions of the wing at these angles of attack. In general, figure 7 also indicates as was shown in reference 2, that, for the angles of attack investigated, the root-fixed spoilers developed greater rolling moments than equal-span tip-fixed spoilers. It is possible that, as a result of the lateral outflow, the inboard-located spoilers on sweptback wings may materially spoil the flow over the outboard wing sections; thereby less lift and larger rolling moments would result.

A method was outlined in reference 2 to estimate the rolling effectiveness of partial-span spoilers from the data of inboard and outboard spoiler segments. This method has been applied to a partial-span spoiler used in the present investigation and the estimated results are compared in figure 8 to the measured rolling-moment coefficients of the $0.63\frac{b}{2}$-span plain spoiler. The results show good agreement between the estimated and measured values of C_l throughout the angle-of-attack range.

Figures 16 to 18 show that the spoilers resulted, as was expected, in decreased lift, increased drag, and unstable pitching-moment trim shifts at the angles of attack investigated. The unfavorable spoiler effects on the longitudinal characteristics increased with spoiler span and were greatest for the flapped-wing configurations. The tip-fixed spoilers produced favorable yawing characteristics throughout the angle-of-attack range for all spoiler spans and wing configurations. The root-fixed spoilers, however, resulted in adverse yaw for the smaller span spoilers with the greatest effects occurring at the higher angles of attack and for the flapped-wing configurations.

Effect of spoiler projection.- For the basic wing configuration the rolling moments produced by the spoilers are nearly linear for spoiler projections up to about 0.05c' (fig. 9). For greater projections up to 0.10c', the spoiler effectiveness decreased and the maximum value of C_l was attained at an angle of attack of 6.9°. At 16.1°, which is approximately the angle corresponding to $0.85C_{L_{max}}$, the rolling-moment coefficient produced by the spoiler was 77 percent of the maximum value obtained. Although no data have been obtained for small spoiler projections (below 0.02c'), it is conceivable that there may exist a region of spoiler ineffectiveness and possible rolling moments in the opposite direction

(adverse roll). For the flapped-wing configuration a linear variation of the spoiler rolling moment occurs for most of the spoiler-projection range investigated. The maximum rolling-moment coefficient occurred at an angle of attack of 11.9°.

The yawing and longitudinal moments and forces were reduced approximately in proportion to the reduction in spoiler projection for the basic wing with the percentage reduction being smaller for the flapped-wing configuration than for the plain wing (figs. 16 and 18).

Effect of spoiler chordwise location and perforation.- The basic and flapped-wing results given in figure 10 indicate that, at the angle of attack corresponding to $0.85C_{L_{max}}$ (16.4° for the basic wing and 15.5° for the flapped wing), the rolling-moment coefficients were essentially independent of spoiler chordwise location. As indicated from tuft observations, the flow at the spoiler locations was generally disturbed over a large portion of the wing, and for the basic wing configuration the flow at the tip sections was stalled. The yawing-moment coefficients at $0.85C_{L_{max}}$ indicate that the 50-percent chordwise-located spoiler produced almost twice the yawing moment that the rearward-located spoiler produced. The drag coefficients of figure 19 show the drag of the forward-located spoiler to be approximately 10 percent greater than that for the 70-percent chordwise-located spoiler.

At $0.85C_{L_{max}}$, chordwise location had no appreciable effect on the rolling moments obtained. However, at the higher angles of attack, from $0.85C_{L_{max}}$ to $C_{L_{max}}$, the rolling-moment coefficients of the forward-located spoiler were slightly greater than the rolling power of the 70-percent chordwise-located spoiler. At the low and moderate angles of attack the trend of the rolling-moment curves was opposite; that is, the rearward-located spoiler produced greater roll than the 50-percent chordwise-located spoiler. Similar results were obtained on several 42° sweptback wings with NACA 64_1-112 airfoil sections and are reported in references 2 and 4.

A few exploratory tests were conducted to determine the effects of a perforated spoiler on the aerodynamic characteristics of the model with and without flaps. In general, the data of figure 19 indicate no appreciable differences in the lateral or longitudinal characteristics of the model at high lift coefficients with either the plain or perforated type of spoiler. As was previously noted, at the high angles of attack the spoilers were located in regions of disturbed flow and their effectiveness was limited. In the low and moderate angles of attack, however, the perforated spoiler produced greater rolling moments than the plain spoiler when located at the 0.50c station. The air flow through the perforations may have resulted in a greater detrimental effect on the

[redacted]

section pressure distribution than the plain-type spoiler. The decreased drag, due to spoiler perforation, resulted in less favorable yawing moments at the low and moderate angles of attack; however, both types of spoilers produced adverse yaw at the stall. As a result of the decreased lift and drag in the angle-of-attack range below the stall, the perforated spoilers caused positive longitudinal trim shifts for all configurations.

Comparison of Ailerons and Spoilers

In order to compare the lateral-control effectiveness of ailerons and spoilers, a brief comparison of the lateral-control characteristics of the model with an aileron $\left(0.45\frac{b}{2}\text{ span}\right)$ and two 0.10c' tip-fixed spoilers $\left(0.856\frac{b}{2}\text{ and }0.448\frac{b}{2}\text{ span}\right)$ is presented. It should be noted that there are no hinge-moment data available and that a complete evaluation would require comparisons of such data. For the basic wing configuration, figure 11 shows that a total aileron deflection of 48° would be required to produce rolling moments comparable to those produced by the $0.856\frac{b}{2}$-span spoiler between 7° and 14° angle of attack and greater rolling moments below and above this angle-of-attack range. If the aileron deflection angle was limited to 30°, however, the rolling moments of the spoiler configuration would be much greater than the rolling moments of the aileron throughout the angle-of-attack range. The rolling moments produced by the ailerons may also be decreased as a result of the adverse yaw (fig. 11(b)) which occurred for all aileron-control deflection angles.

For the configuration with extensible leading-edge flaps, combined with plain trailing-edge flaps, the rolling moments of a $0.856\frac{b}{2}$-span spoiler was greater than the rolling effectiveness of the half-span aileron at the largest deflection angle (56°) investigated. A smaller span spoiler $\left(0.448\frac{b}{2}\right)$ was, therefore, considered and it can be seen that 32° of aileron deflection would produce rolling moments similar to that of the partial-span spoiler throughout the angle-of-attack range. Comparison based on an angle of attack corresponding to $0.85C_{L_{max}}$, however, indicates that the spoiler rolling moment is approximately 45 percent lower than that for the aileron deflected 56°. The difference in rolling moment between the aileron and the spoiler may be reduced, inasmuch as the adverse yaw produced by the ailerons would effectively decrease the aileron rolling capabilities.

CONCLUDING REMARKS

The results of the Langley full-scale-tunnel investigation of a 47.5° sweptback-wing - fuselage combination with several lateral-control devices are summarized as follows:

1. The aileron effectiveness of small-span ailerons located inboard of the 77.5-percent-span station was greater than the aileron effectiveness of equal-span ailerons located at the wing tips. For large-span ailerons, the aileron effectiveness at 85 percent of the maximum lift was equivalent to the sum of the effectiveness of the component aileron spans.

2. The aileron effectiveness of the model with the thick trailing-edge and original contour ailerons was essentially the same in the high angle-of-attack range. The drag increments near the stall due to the thick ailerons were small.

3. In general, for the angles of attack investigated, spoilers located in the region of the plane of symmetry developed greater rolling moments than equal-span spoilers located at the wing tip. The addition of the spoilers resulted in positive longitudinal trim shifts at the angles of attack investigated.

4. Increasing spoiler projection increased the rolling moments through most of the spoiler-projection range investigated.

5. The rolling moments produced by a partial-span spoiler located at the midspan were essentially independent of spoiler chordwise location at the angle of attack corresponding to 85 percent of the maximum lift. A perforated spoiler did not change the lateral or longitudinal characteristics of the model at the high angles of attack.

6. The comparison between aileron and spoilers shows that large deflection angles of a half-span aileron would produce rolling moments equivalent to a moderate-span spoiler located in the region of the plane of symmetry.

7. The yawing characteristics for all aileron configurations were unfavorable; whereas, only the small-span spoilers located at the wing root sections resulted in adverse yaw, especially at high angles of attack.

Langley Aeronautical Laboratory
National Advisory Committee for Aeronautics
Langley Air Force Base, Va.

[redacted]

REFERENCES

1. Langley Research Staff (Compiled by Thomas A. Toll): Summary of Lateral Control Research. NACA Rep. 868, 1947.

2. Bollech, Thomas V., and Pratt, George L.: Effects of Plain and Step Spoiler Location and Projection on the Lateral Control Characteristics of a Plain and Flapped 42° Sweptback Wing at a Reynolds Number of 6.8×10^6. NACA RM L9L20a, 1950.

3. Fischel, Jack, and Schneiter, Leslie E.: An Investigation at Low Speed of a 51.3° Sweptback Semispan Wing Equipped with 16.7-Percent-Chord Plain Flaps and Ailerons Having Various Spans and Three Trailing-Edge Angles. NACA RM L8H20, 1948.

4. Schneiter, Leslie E., and Watson, James M.: Low-Speed Wind-Tunnel Investigation of Various Plain-Spoiler Configurations for Lateral Control on a 42° Sweptback Wing. NACA TN 1646, 1948.

5. Pasamanick, Jerome, and Sellers, Thomas B.: Low-Speed Investigation of Leading-Edge and Trailing-Edge Flaps on a 47.5° Sweptback Wing of Aspect Ratio 3.4 at a Reynolds Number of 4.4×10^6. NACA RM L50E02, 1950.

6. Theodorsen, Theodore, and Silverstein, Abe: Experimental Verification of the Theory of Wind-Tunnel Boundary Interference. NACA Rep. 478, 1934.

7. Turner, Thomas R., Lockwood, Vernard E., and Vogler, Raymond D.: Aerodynamic Characteristics at Subsonic and Transonic Speeds of a 42.7° Sweptback Wing Model Having an Aileron with Finite Trailing-Edge Thickness. NACA RM L8K02, 1949.

8. Lange, Roy H.: Full-Scale Investigation of a Wing with the Leading Edge Swept Back 47.5° and Having Circular-Arc and Finite-Trailing-Edge-Thickness Ailerons. NACA RM L9B02, 1949.

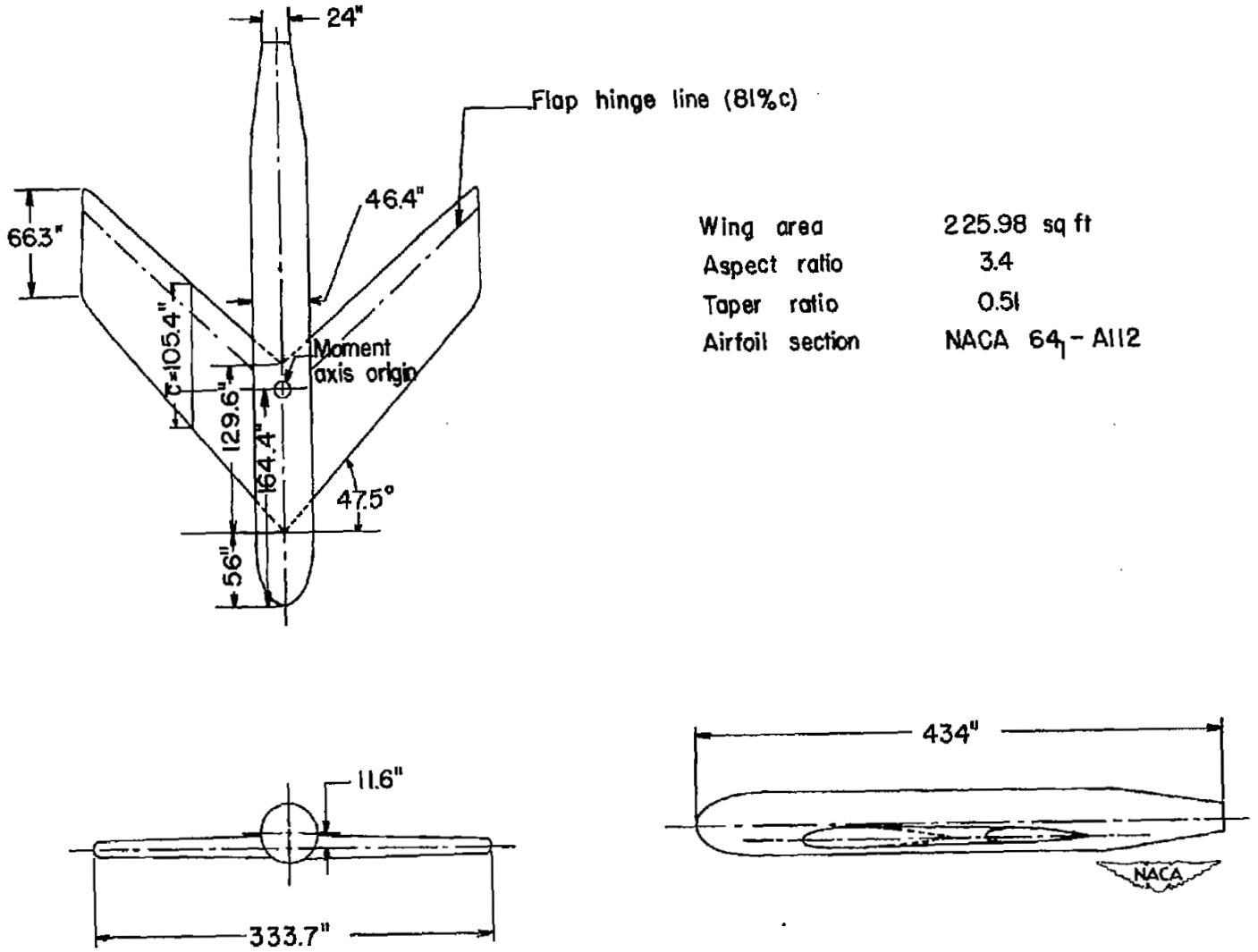

Wing area	225.98 sq ft
Aspect ratio	3.4
Taper ratio	0.51
Airfoil section	NACA 64_1-A112

Figure 1.- Three-view drawing of a 47.5° sweptback-wing - fuselage combination.

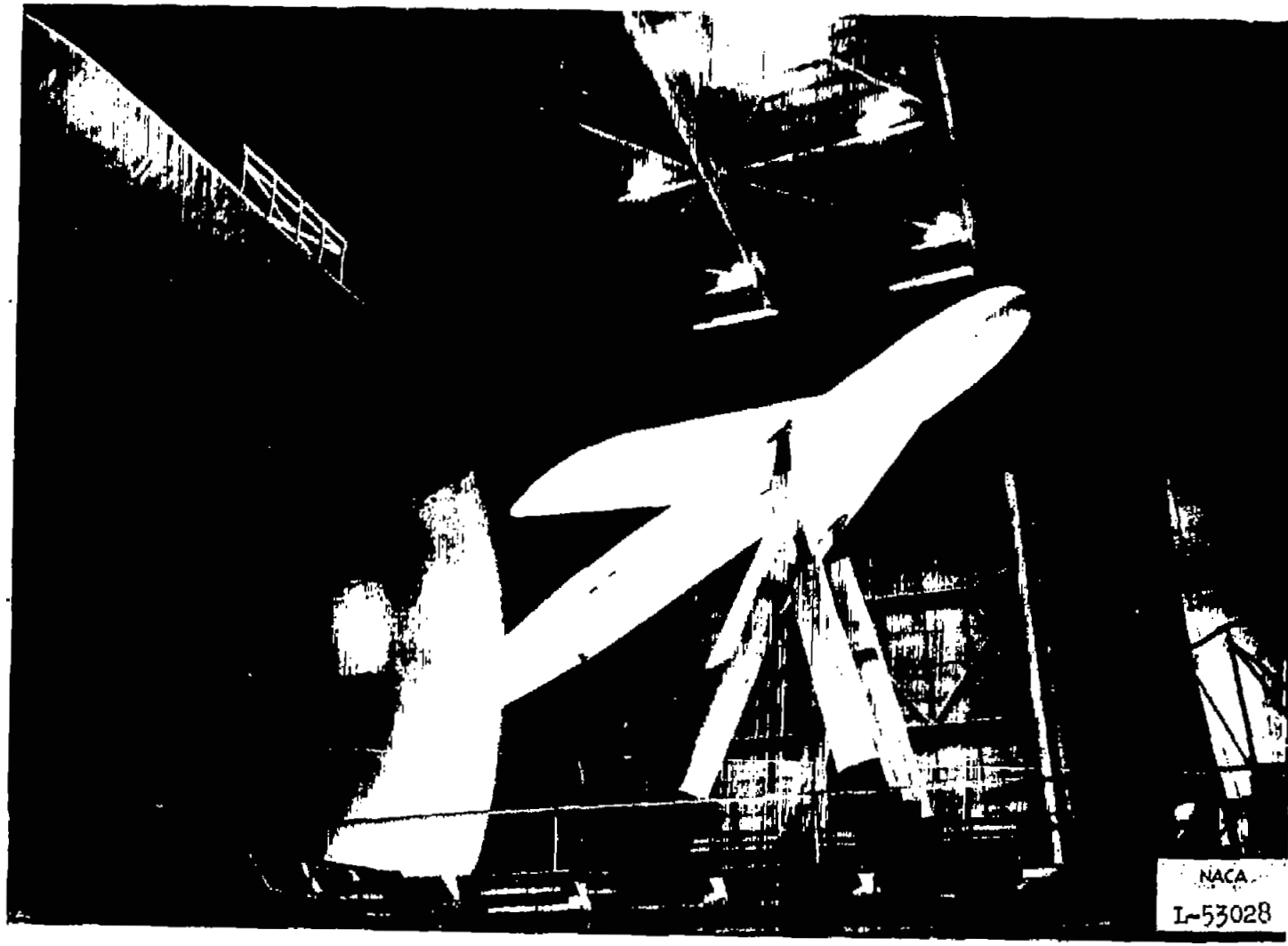

Figure 2.- Three-quarter front view of the 47.5° sweptback-wing model mounted in the Langley full-scale tunnel.

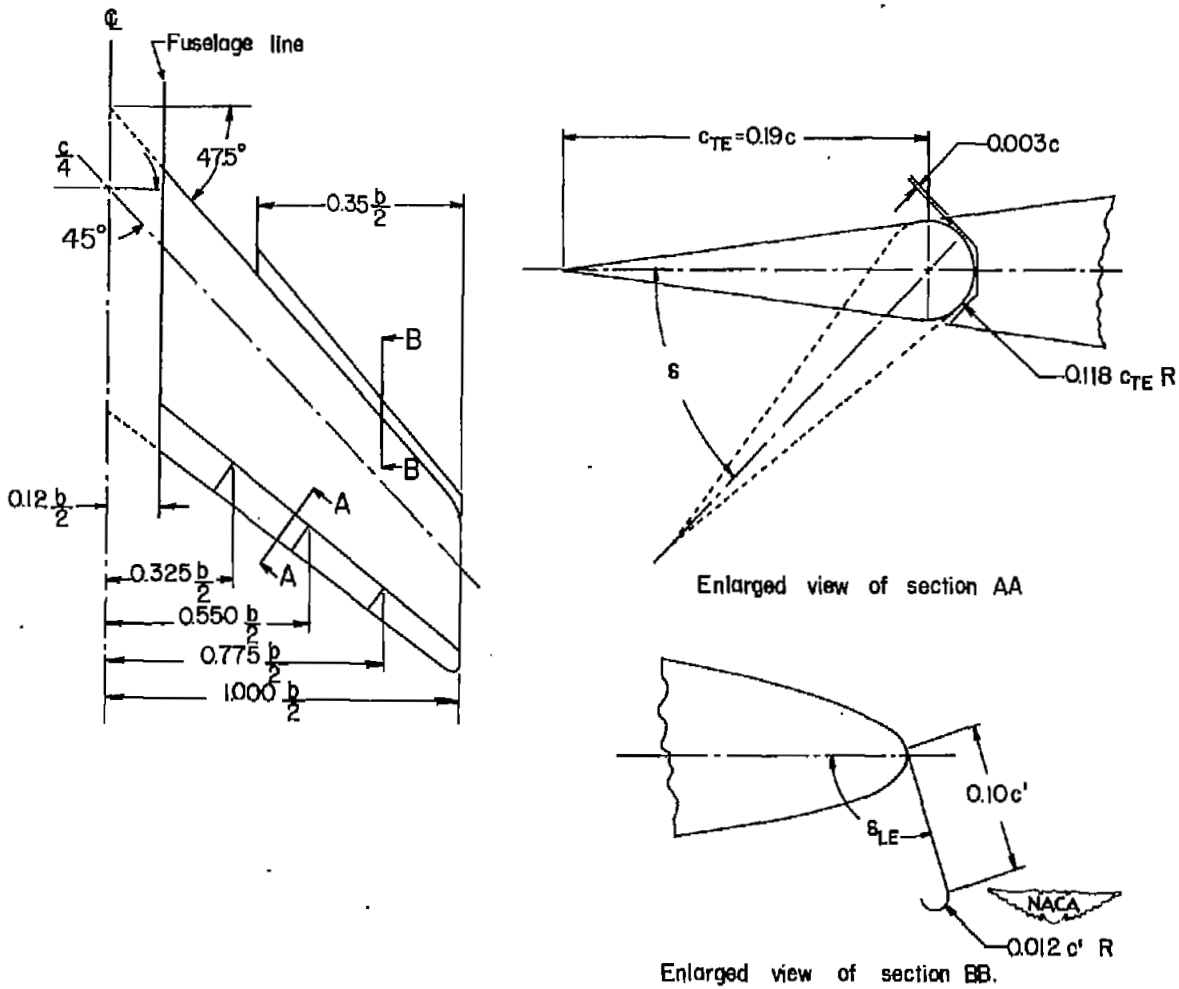

(a) Extensible leading-edge and plain trailing-edge flaps.

Figure 3.- The location and detail dimensions of high-lift and lateral-control devices.

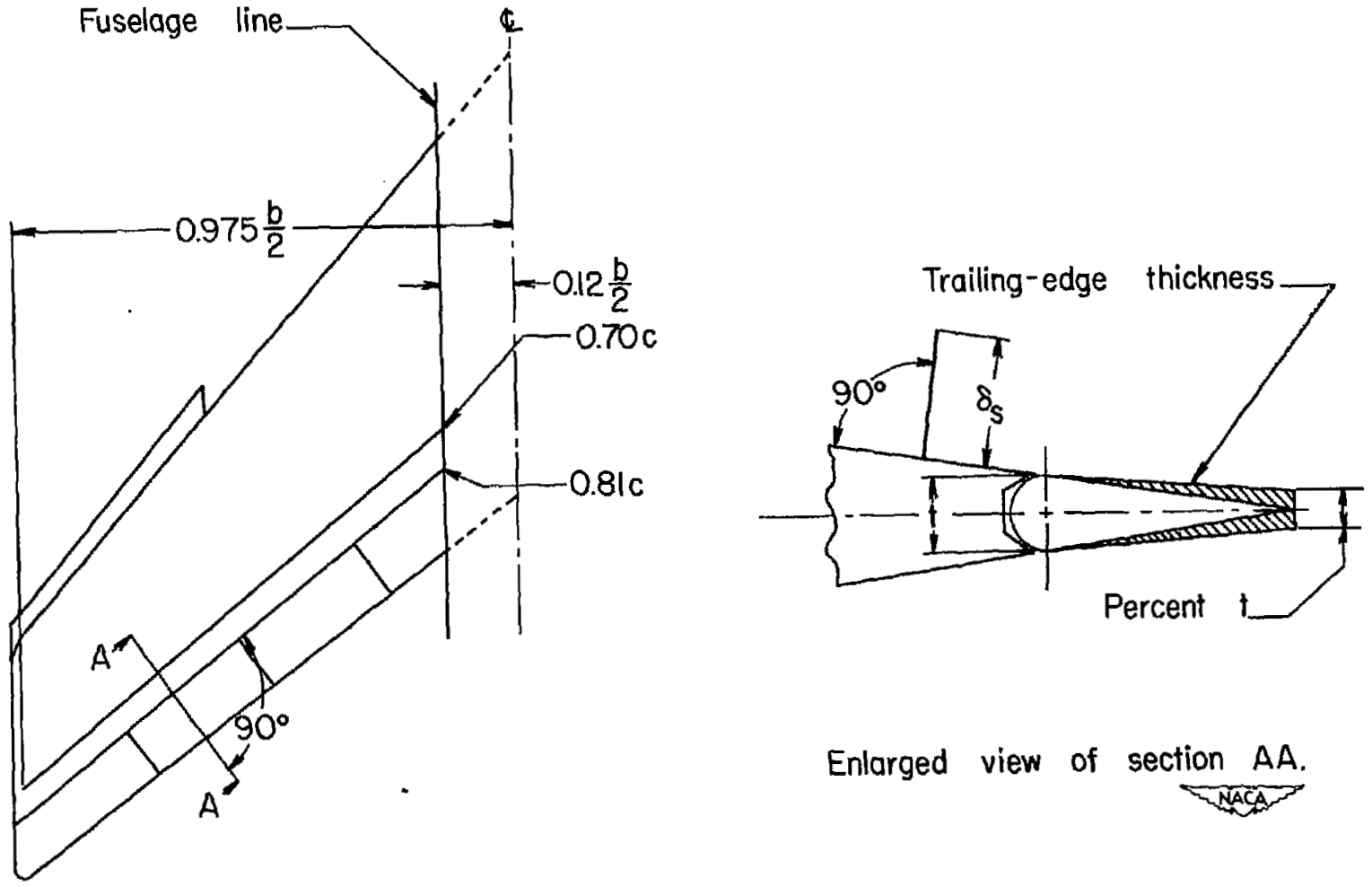

(b) Ailerons and spoilers.

Figure 3.- Concluded.

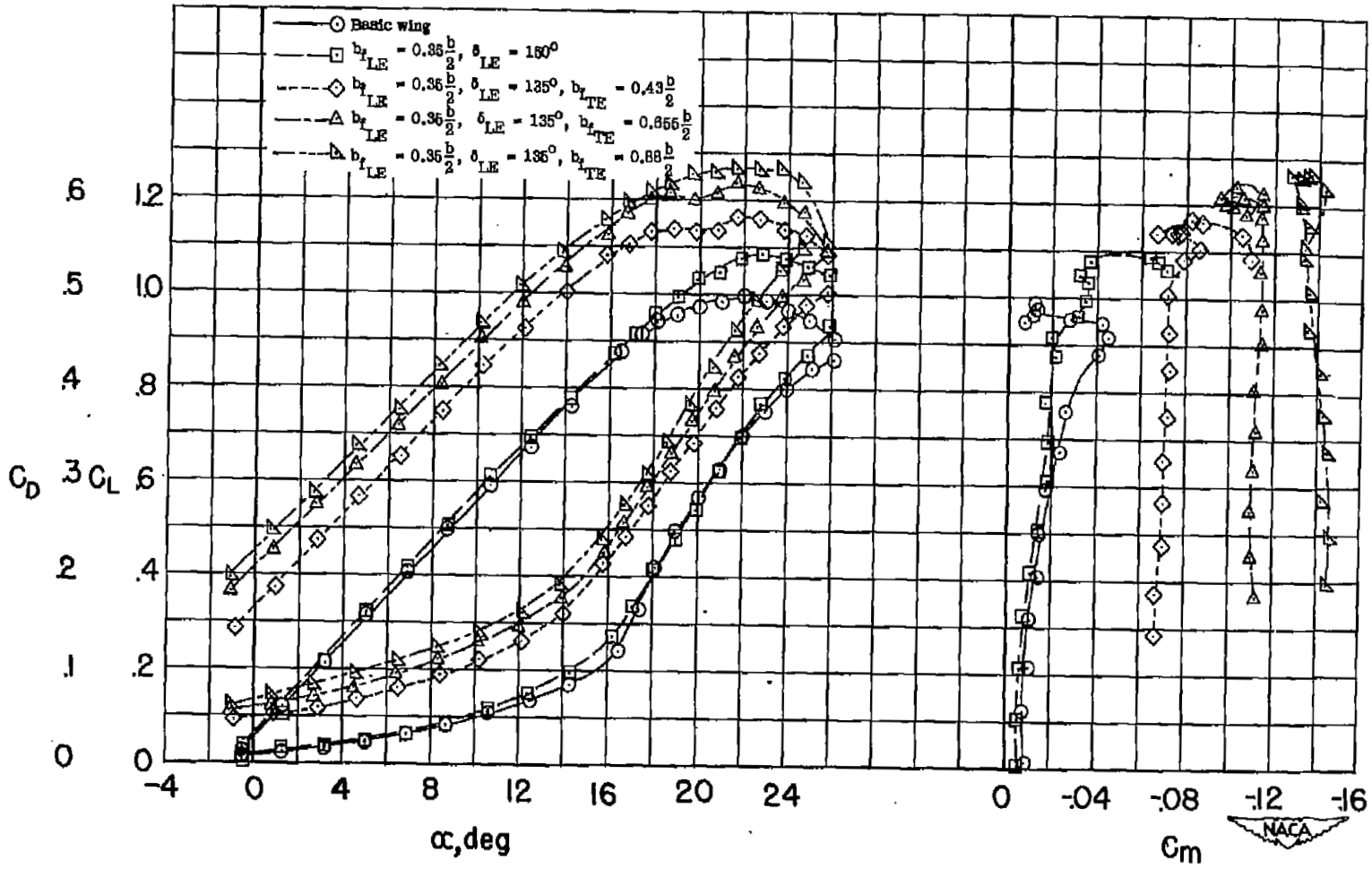

Figure 4.- Longitudinal aerodynamic characteristics of the 47.5° sweptback-wing - fuselage combination with and without flaps. $R = 4.4 \times 10^6$.

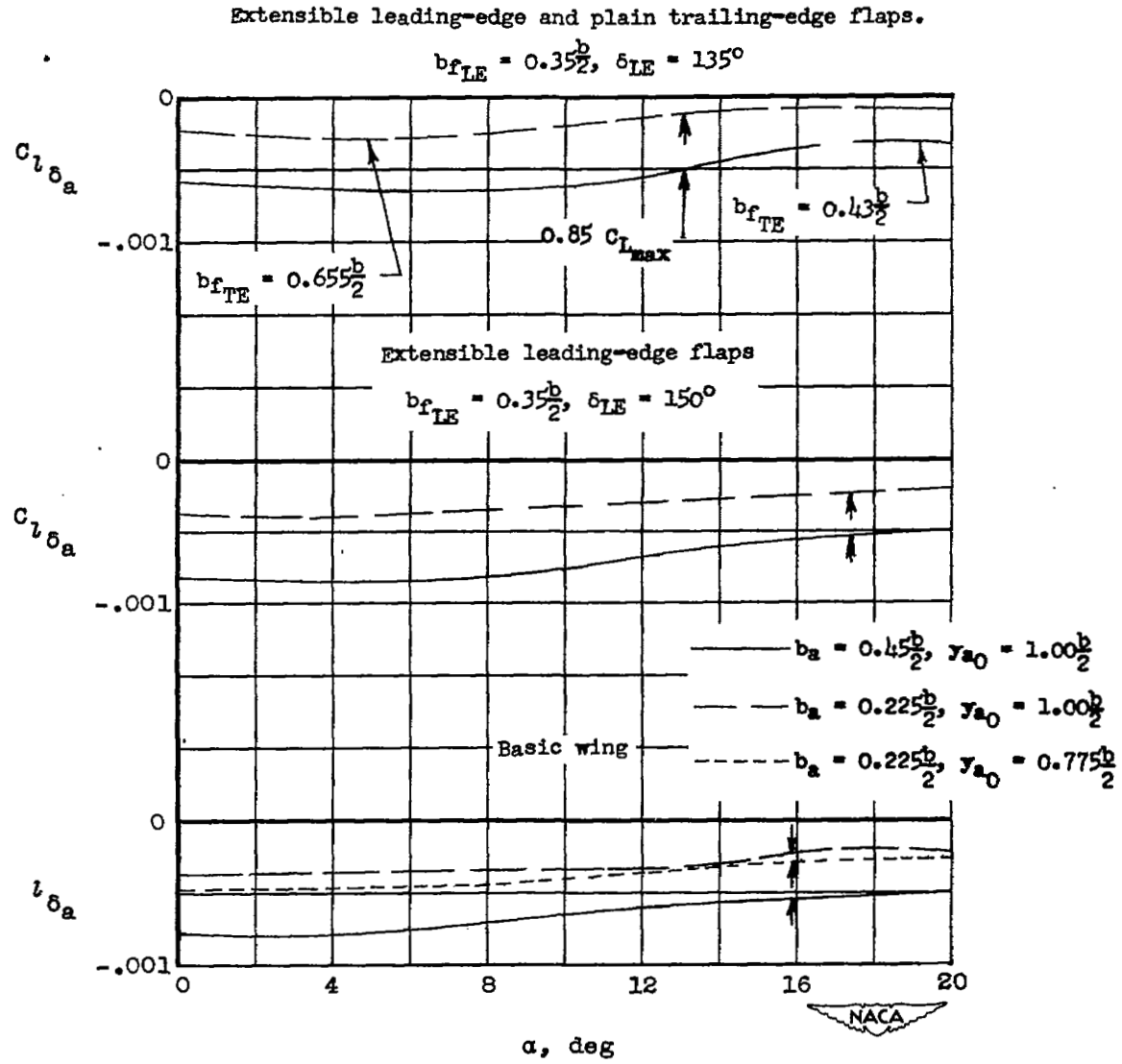

Figure 5.- Effect of aileron span on the aileron-effectiveness parameter for the 47.5° sweptback-wing - fuselage combination with and without flaps. $t = 0$; $R = 4.4 \times 10^6$.

[redacted]

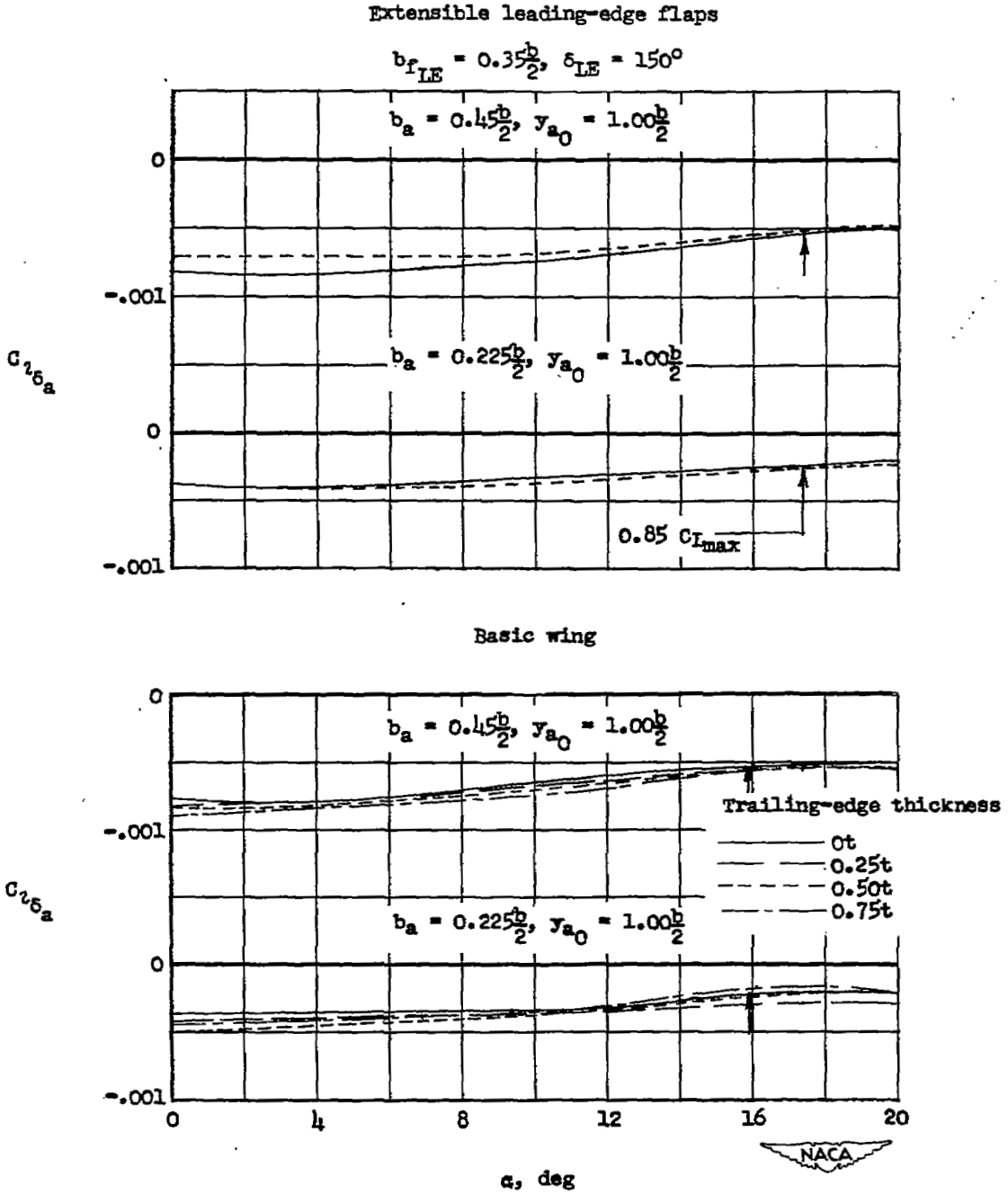

Figure 6.- Effect of aileron trailing-edge thickness and span on the aileron-effectiveness parameter for the 47.5° sweptback-wing - fuselage combination with and without flaps. $R = 4.4 \times 10^6$.

[redacted]

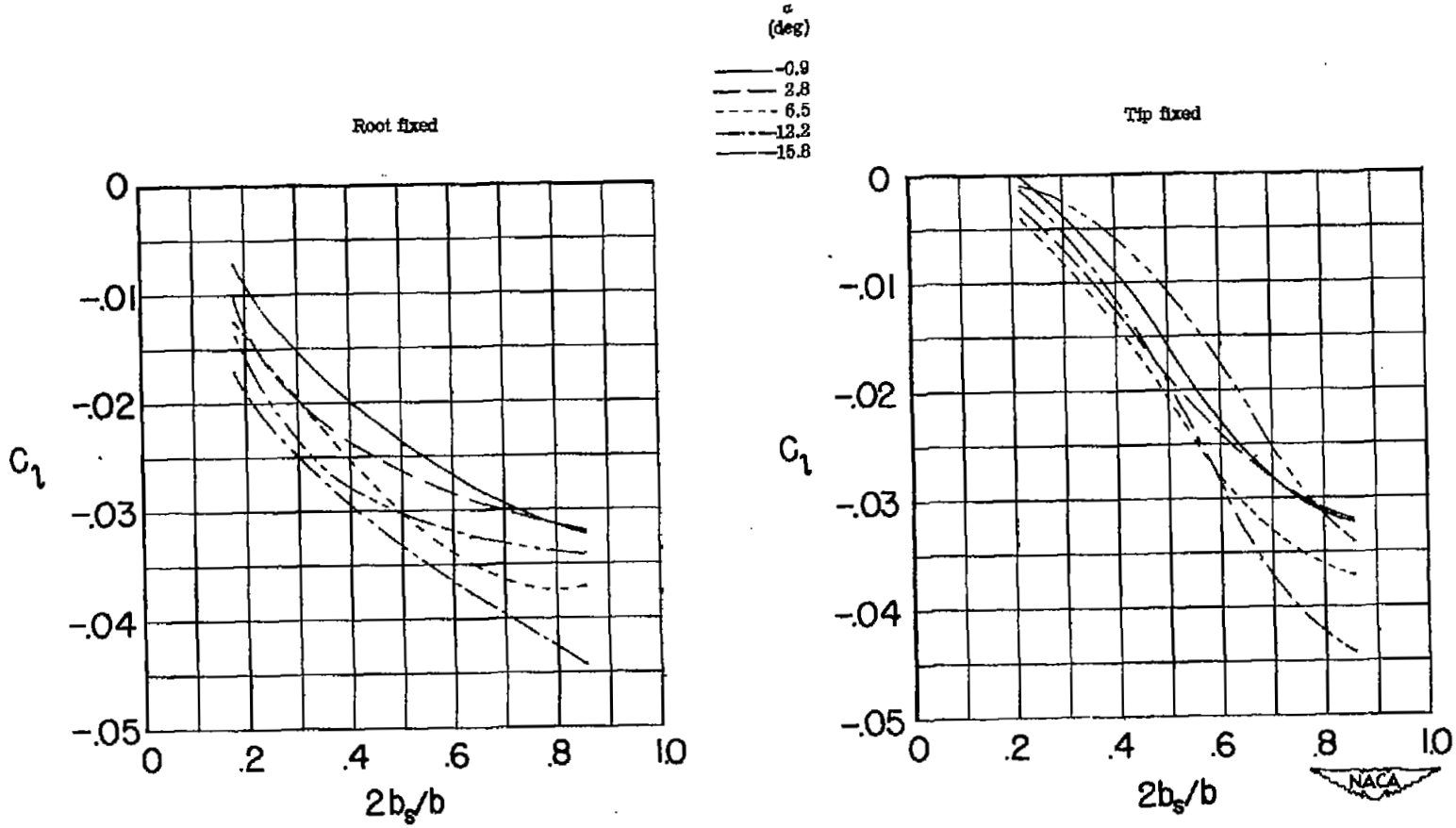

(b) Extensible leading-edge and plain trailing-edge flaps. $b_{f_{LE}} = 0.35\frac{b}{2}$; $\delta_{LE} = 135^{\circ}$; $b_{f_{TE}} = 0.43\frac{b}{2}$.

Figure 7.- Concluded.

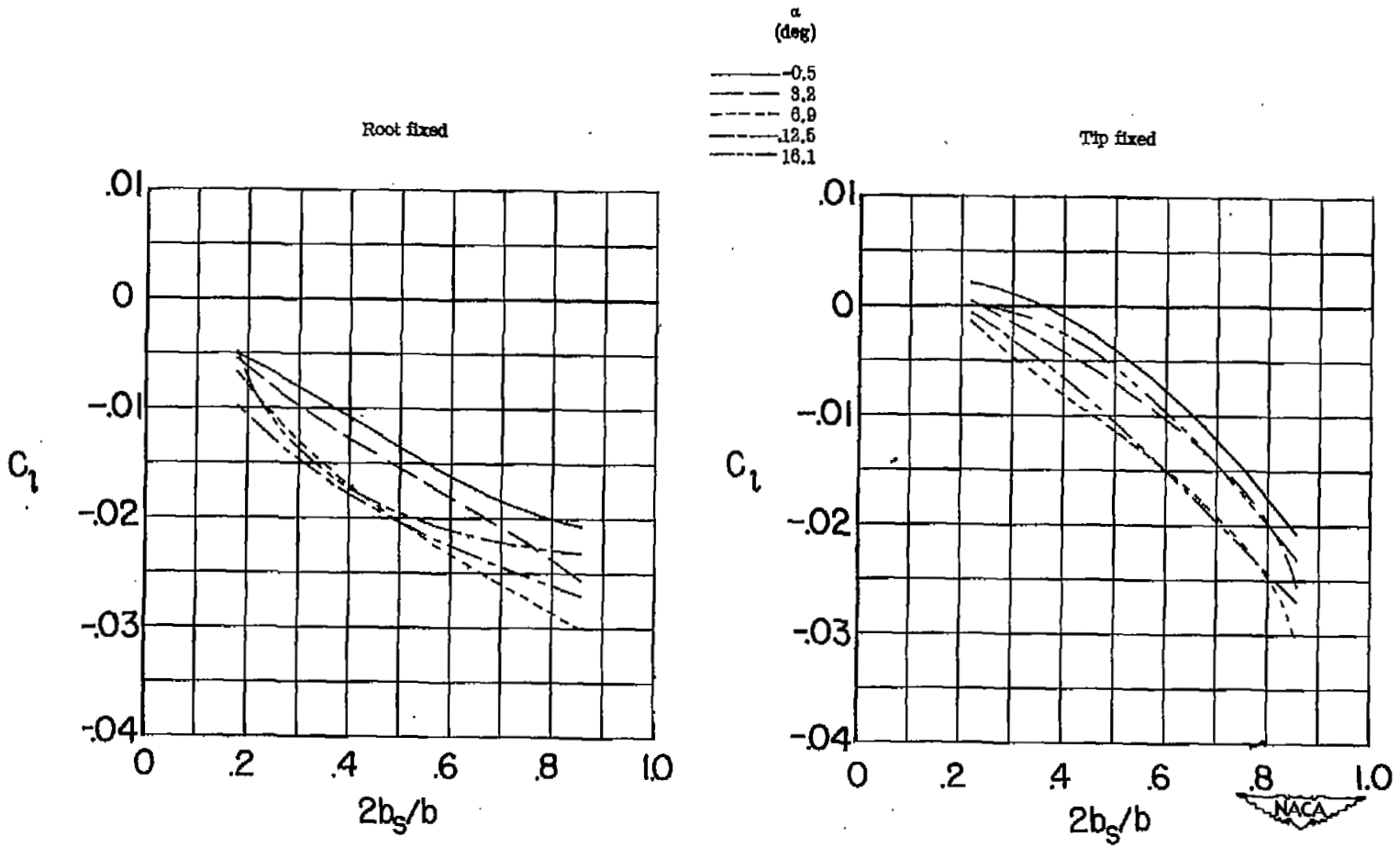

(a) Basic wing.

Figure 7.- Effect of spoiler span on the rolling-moment coefficient for the 47.5° sweptback-wing - fuselage combination. $\delta_s = 0.10c'$; $R = 4.4 \times 10^6$.

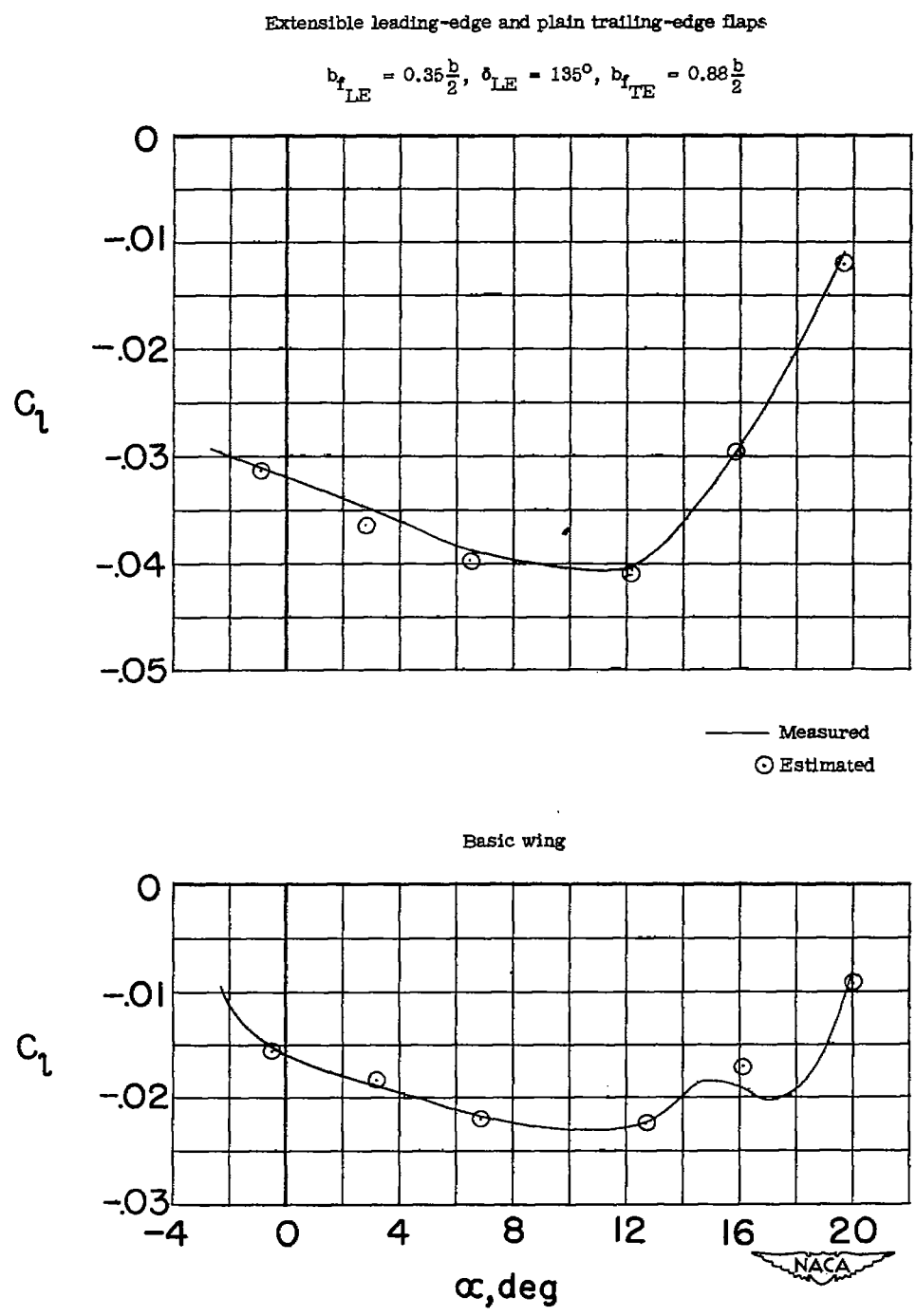

Figure 8.- Comparison of estimated and measured rolling-moment coefficients for a partial-span spoiler. $b_s = 0.63\frac{b}{2}$; $y_{s_o} = 0.863\frac{b}{2}$; $\delta_s = 0.10c'$; $R = 4.4 \times 10^6$.

[redacted]

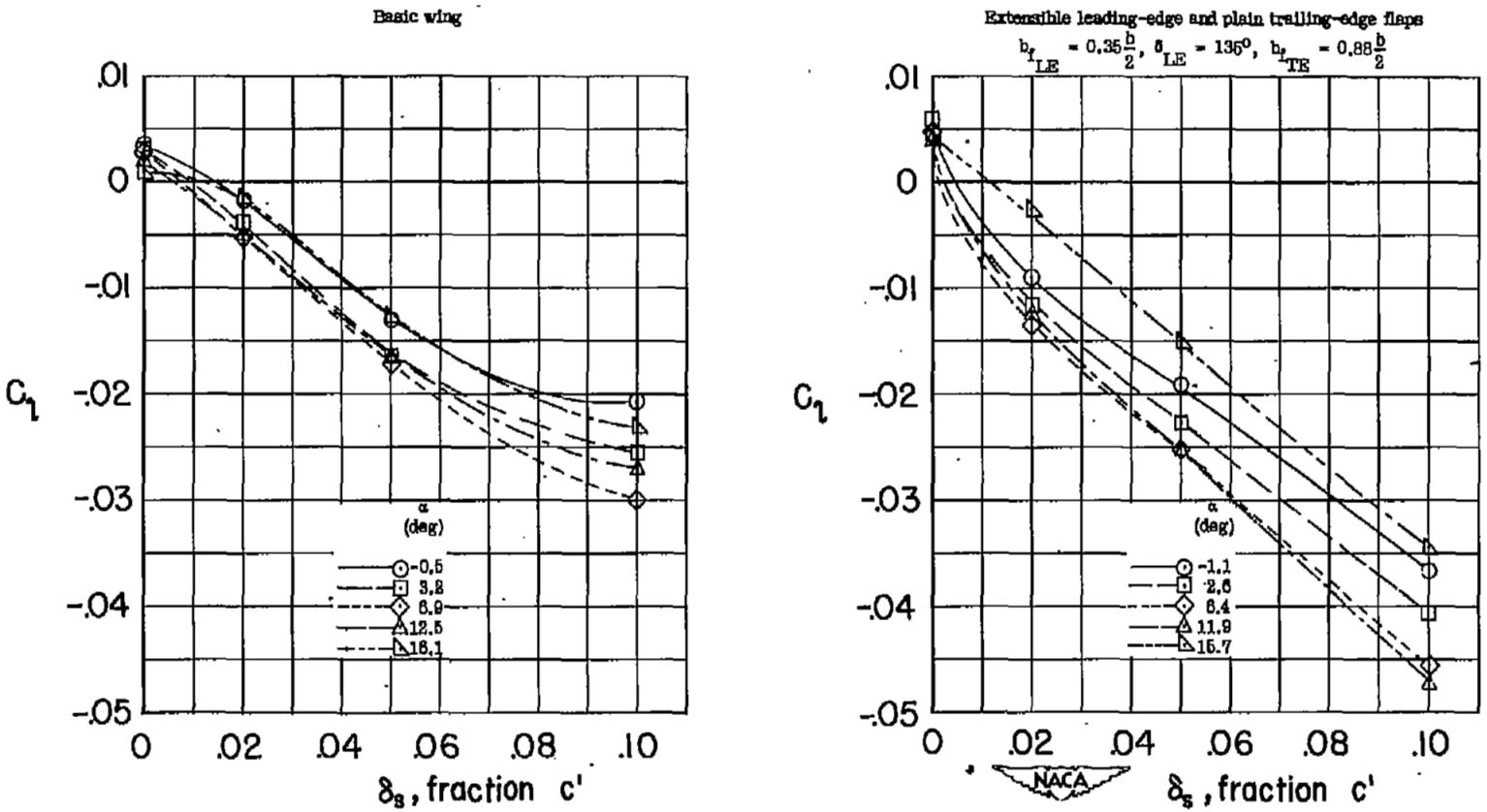

Figure 9.- Effect of spoiler height on the rolling-moment coefficient for the 47.5° sweptback-wing - fuselage combination with and without flaps.

$b_s = 0.856\frac{b}{2}$; $R = 4.4 \times 10^6$.

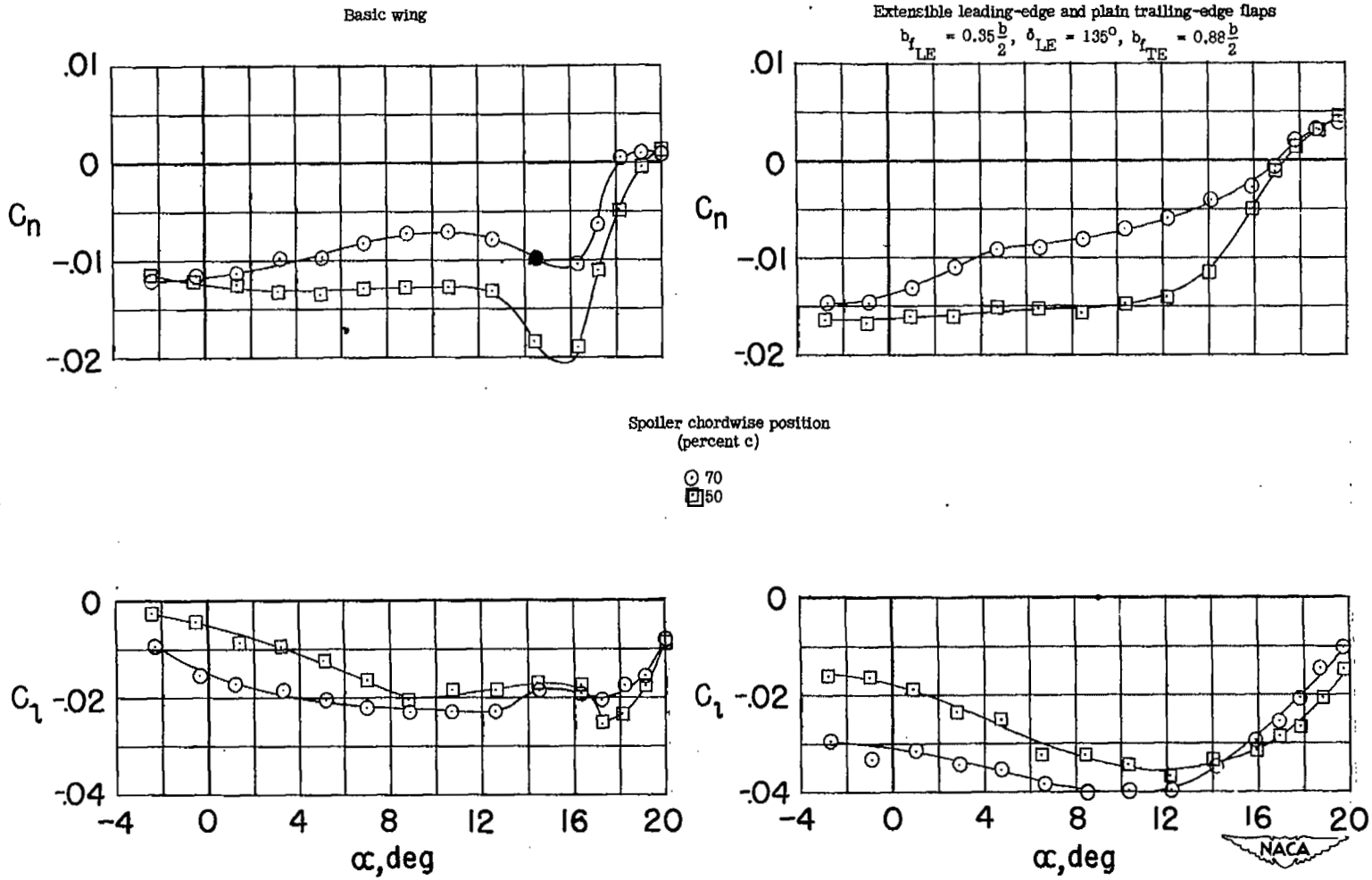

Figure 10.- Effect of spoiler chord location on the lateral characteristics of the 47.5° sweptback-wing - fuselage combination with plain partial-span spoilers. $b_s = 0.63\frac{b}{2}$; $y_{s_o} = 0.863\frac{b}{2}$; $\delta_s = 0.10c'$; $R = 4.4 \times 10^6$.

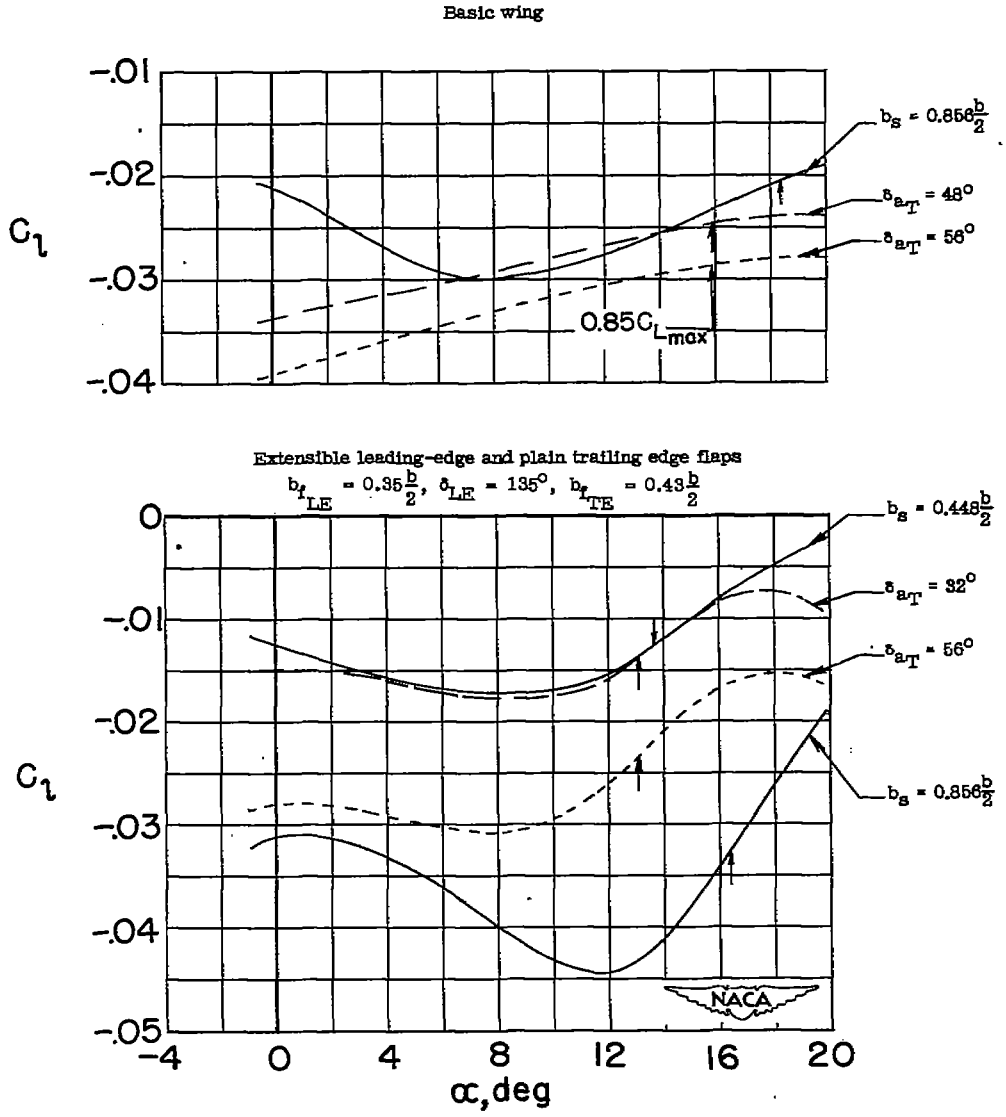

(a) Rolling-moment coefficients.

Figure 11.- Comparison of the lateral control characteristics produced by various aileron deflections and spoiler spans. $\delta_s = 0.10c'$; $b_a = 0.45\frac{b}{2}$; $y_{a_o} = 1.00\frac{b}{2}$; $t = 0$; $R = 4.4 \times 10^6$.

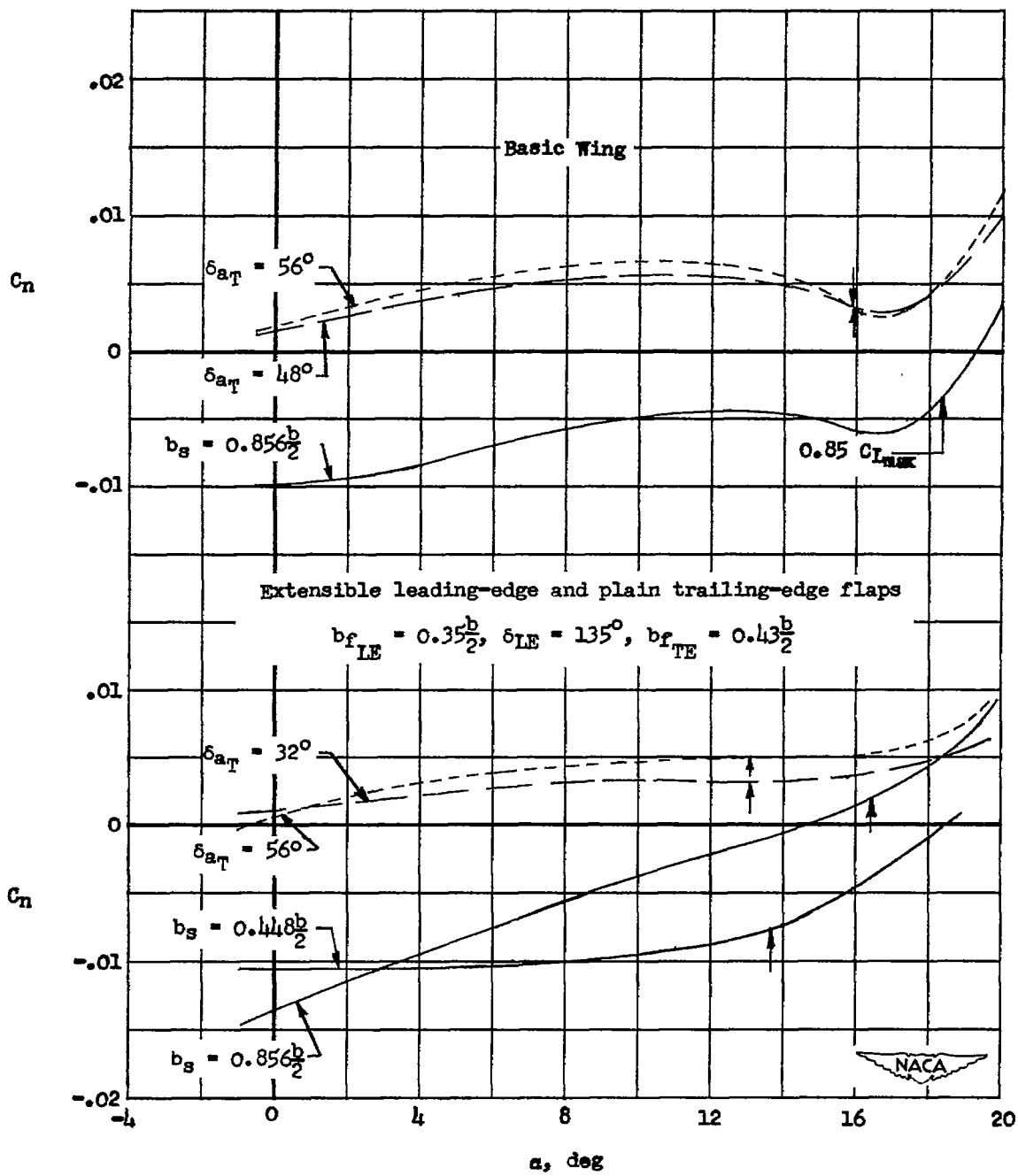

(b) Yawing-moment coefficients.

Figure 11.- Concluded.

[redacted]

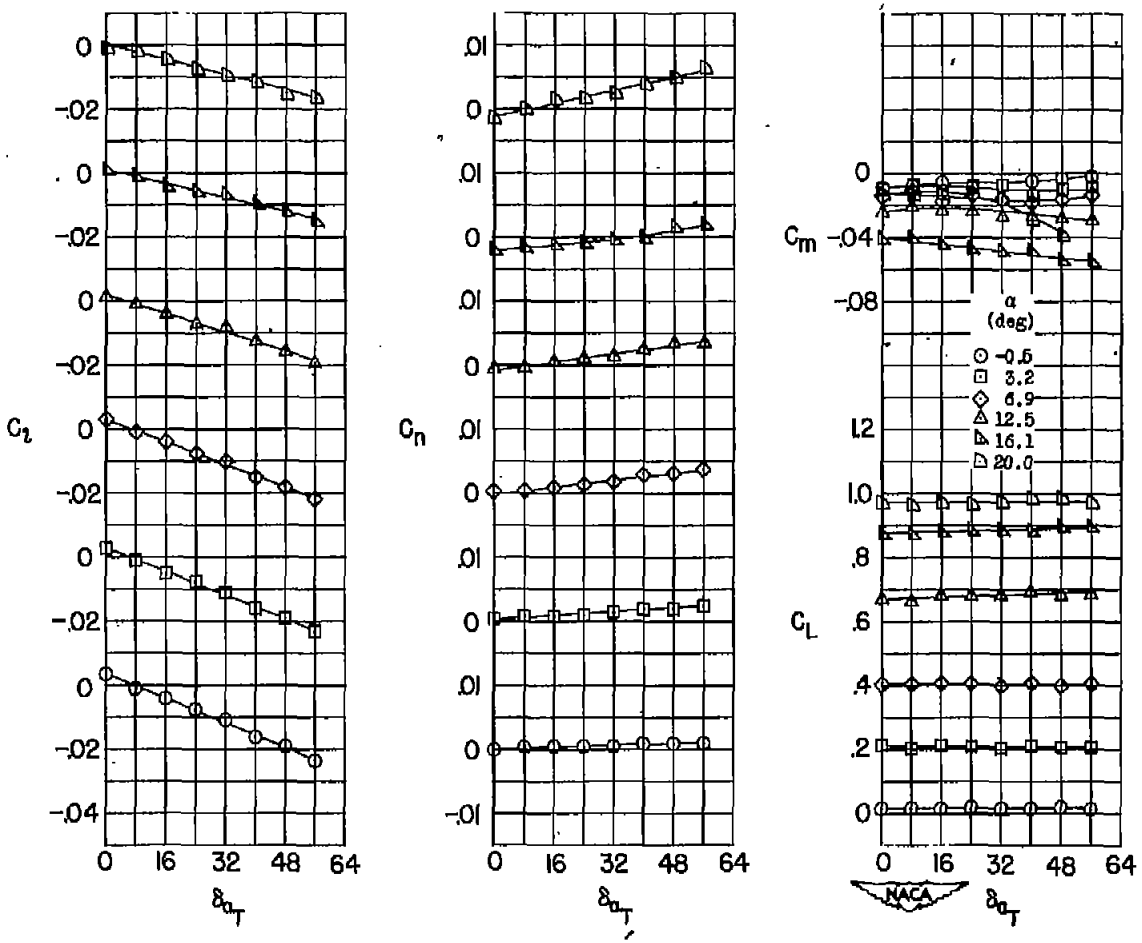

(a) $b_a = 0.225\frac{b}{2}$; $y_{a_o} = 0.775\frac{b}{2}$; $t = 0$.

Figure 12.- Effect of aileron span and trailing-edge thickness on the aerodynamic characteristics of the 47.5° sweptback-wing - fuselage combination. $R = 4.4 \times 10^6$.

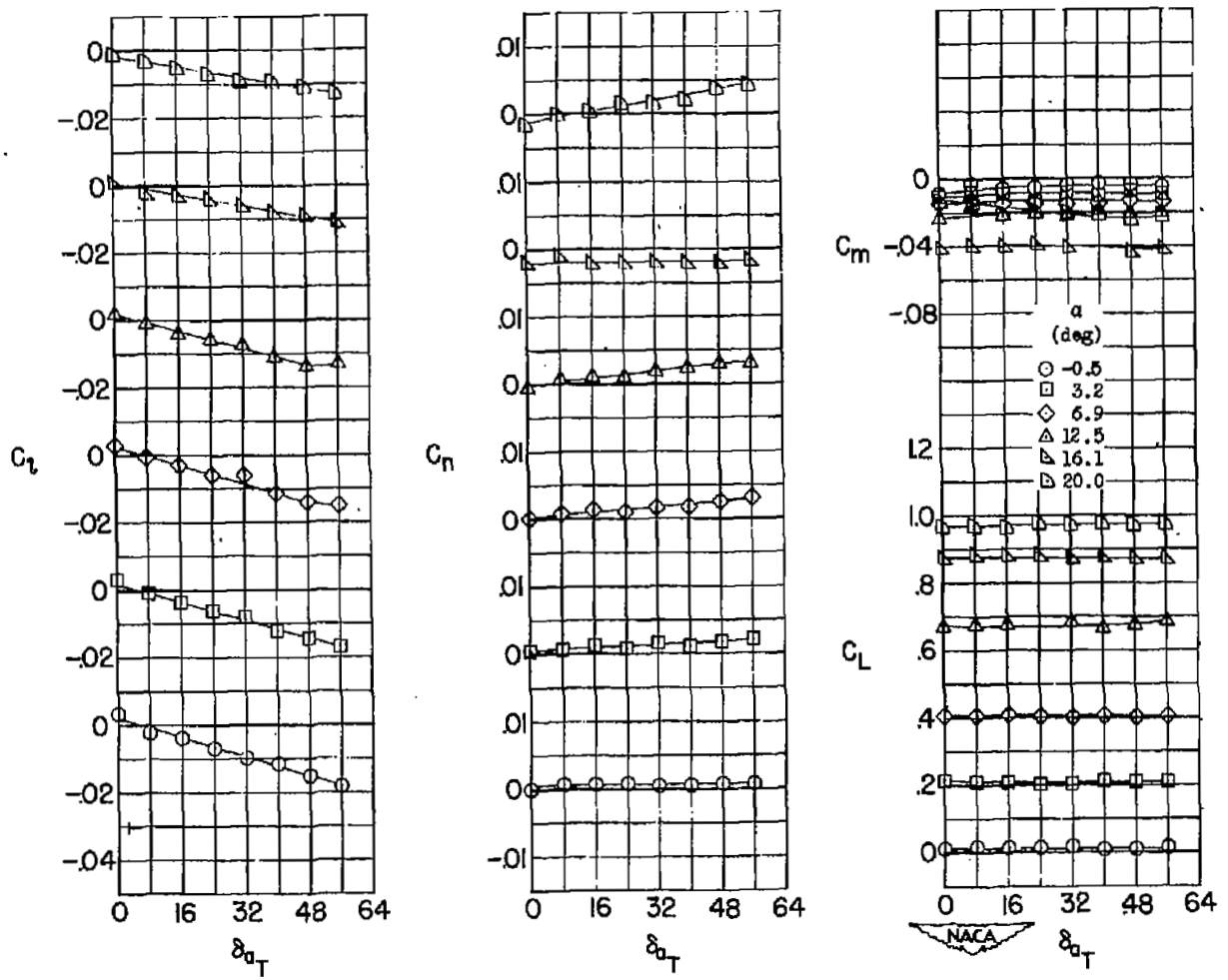

(b) $b_a = 0.225\frac{b}{2}$; $y_{a_o} = 1.00\frac{b}{2}$; $t = 0$.

Figure 12.- Continued.

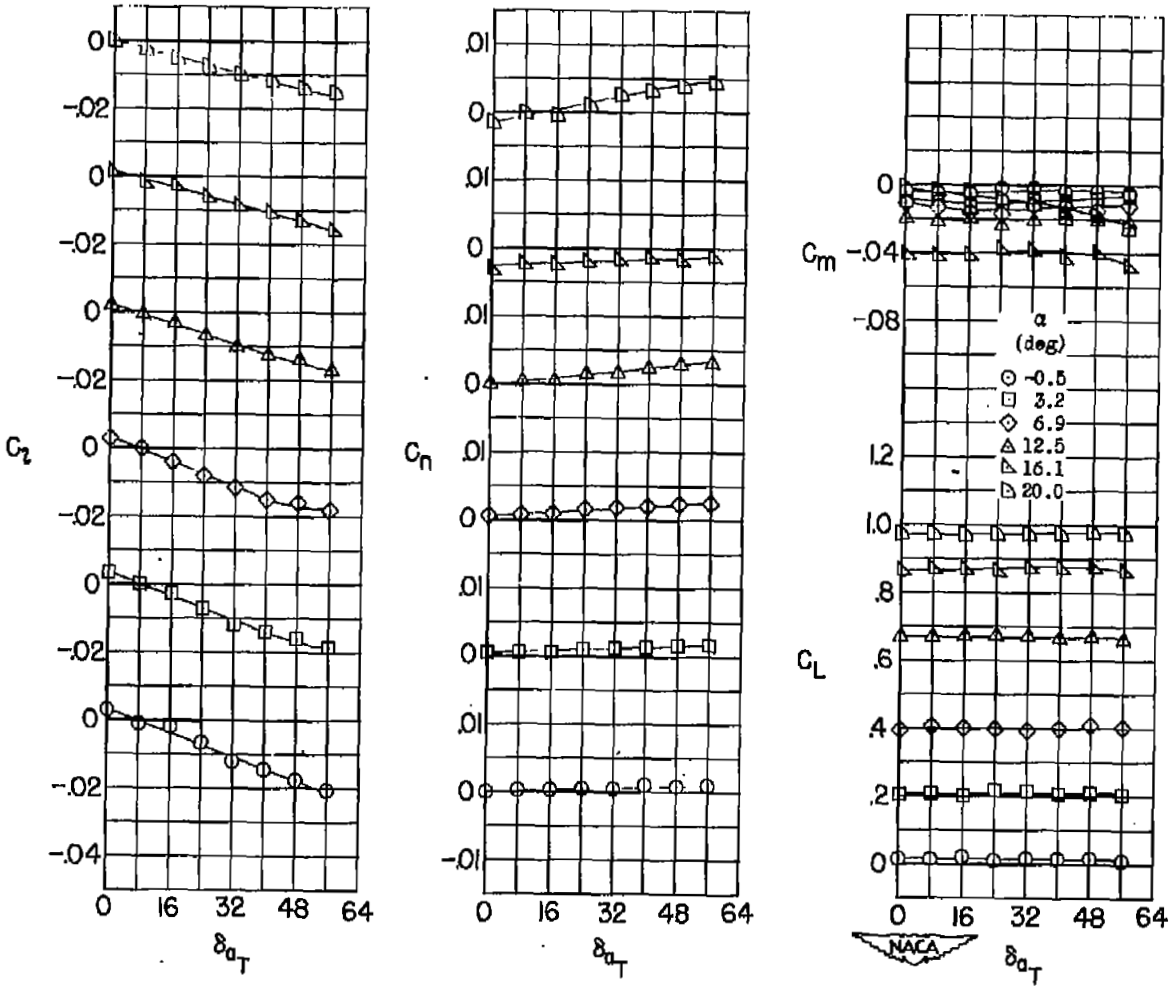

(c) $b_a = 0.225\frac{b}{2}$; $y_{a_o} = 1.00\frac{b}{2}$; $t = 0.25$.

Figure 12.- Continued.

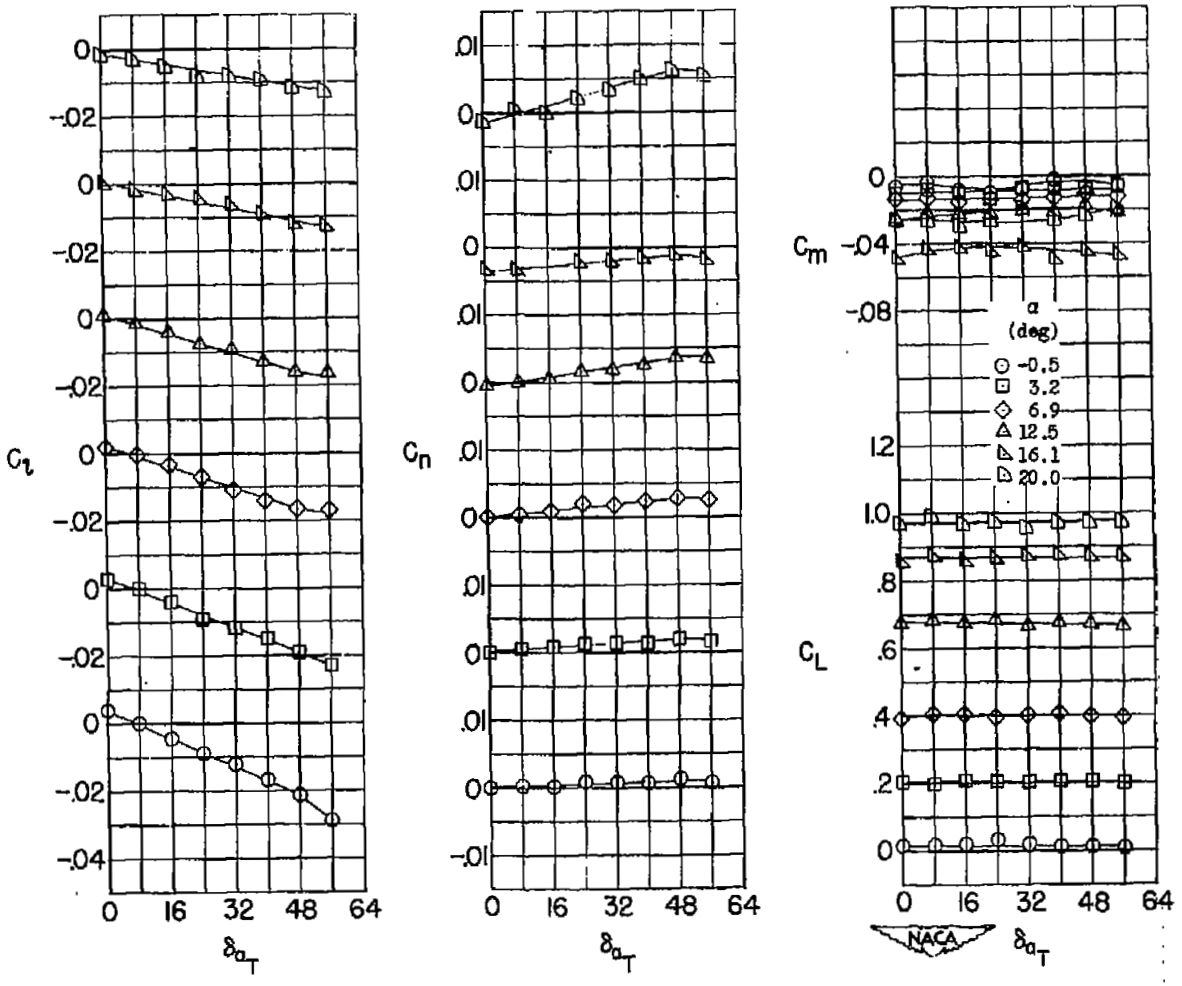

(d) $b_a = 0.225\frac{b}{2}$; $y_{a_o} = 1.00\frac{b}{2}$; $t = 0.50$.

Figure 12.- Continued.

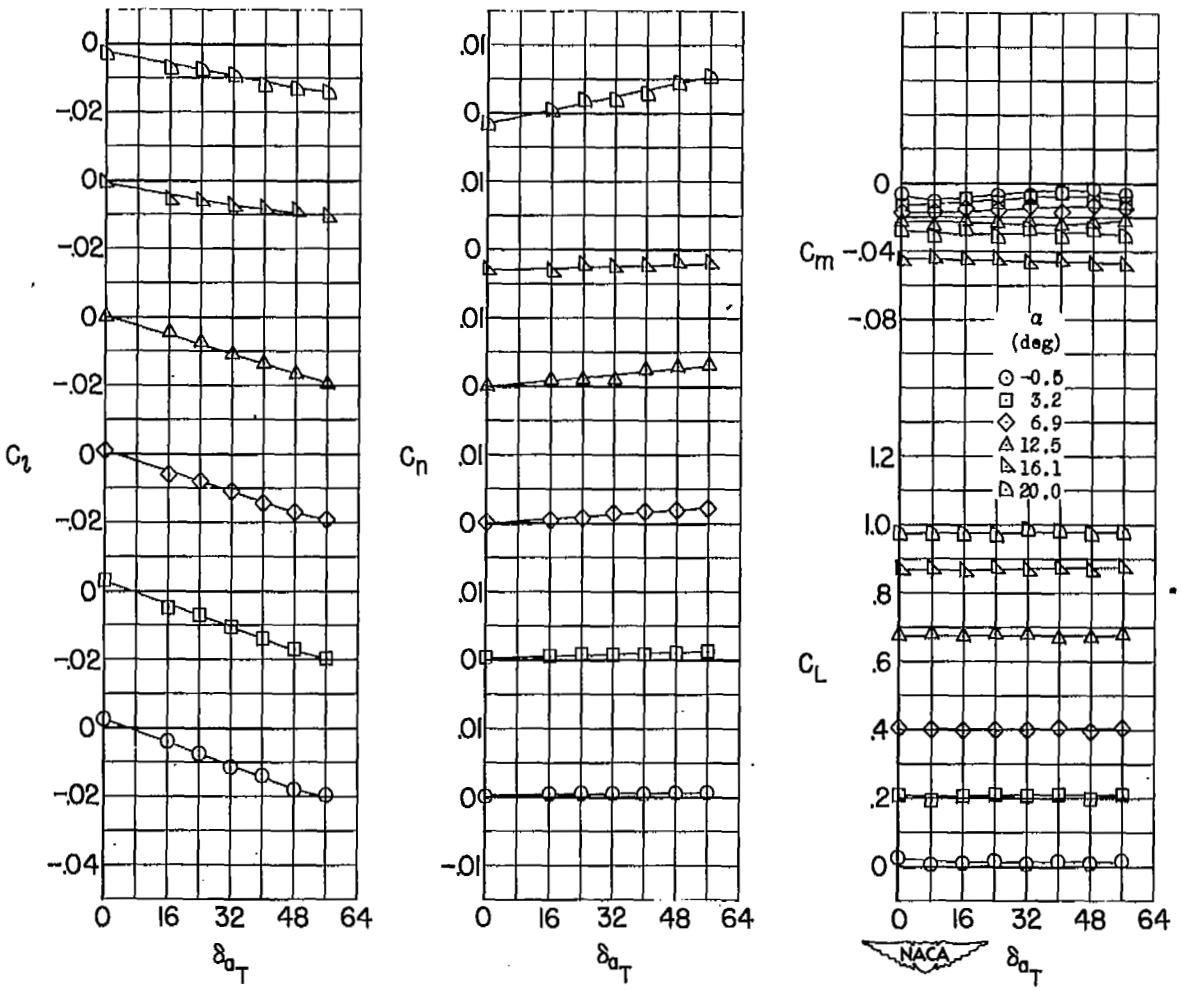

(e) $b_a = 0.225\frac{b}{2}$; $y_{a_o} = 1.00\frac{b}{2}$; $t = 0.75$.

Figure 12.- Continued.

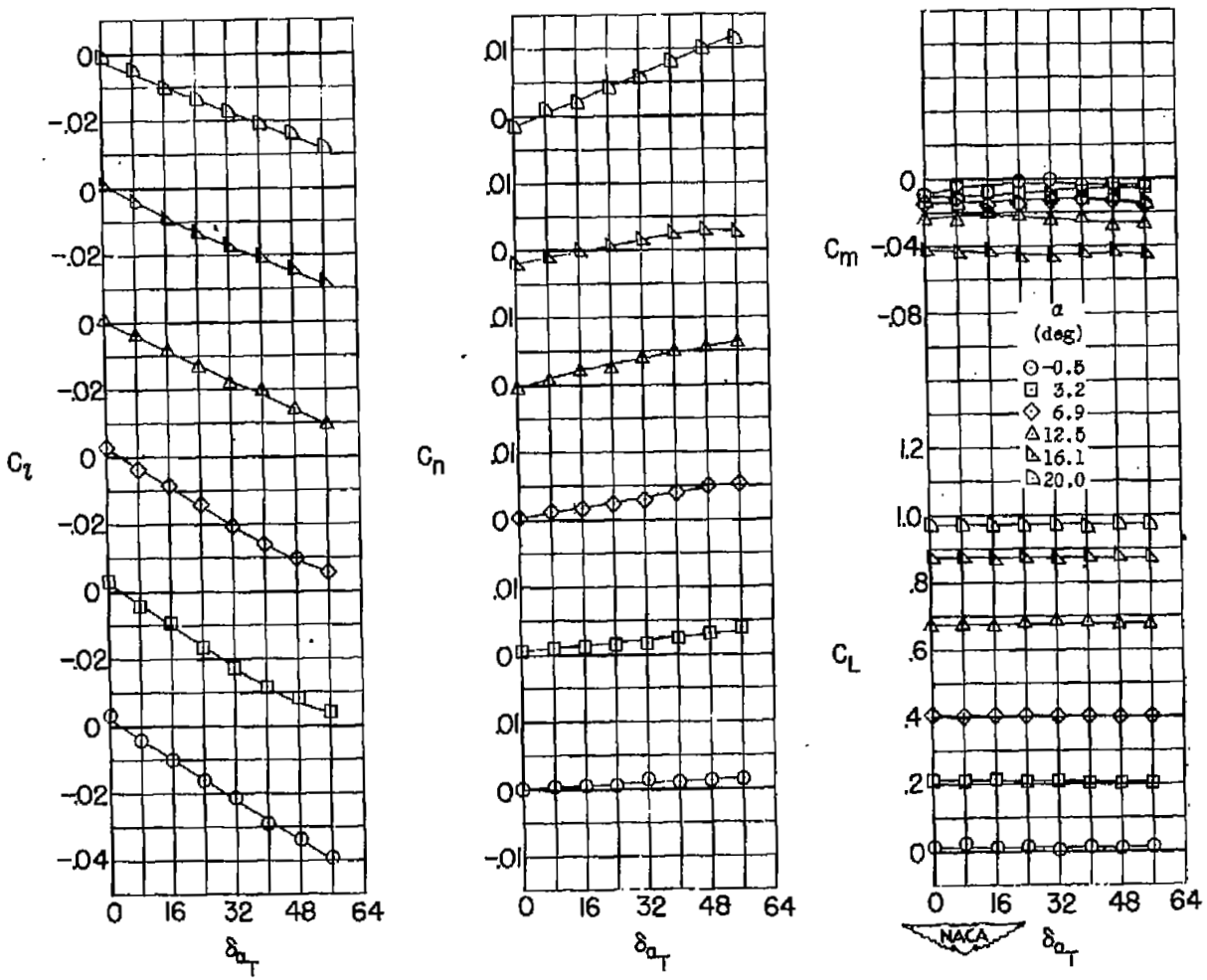

(f) $b_a = 0.45\frac{b}{2}$; $y_{a_o} = 1.00\frac{b}{2}$; $t = 0$.

Figure 12.- Continued.

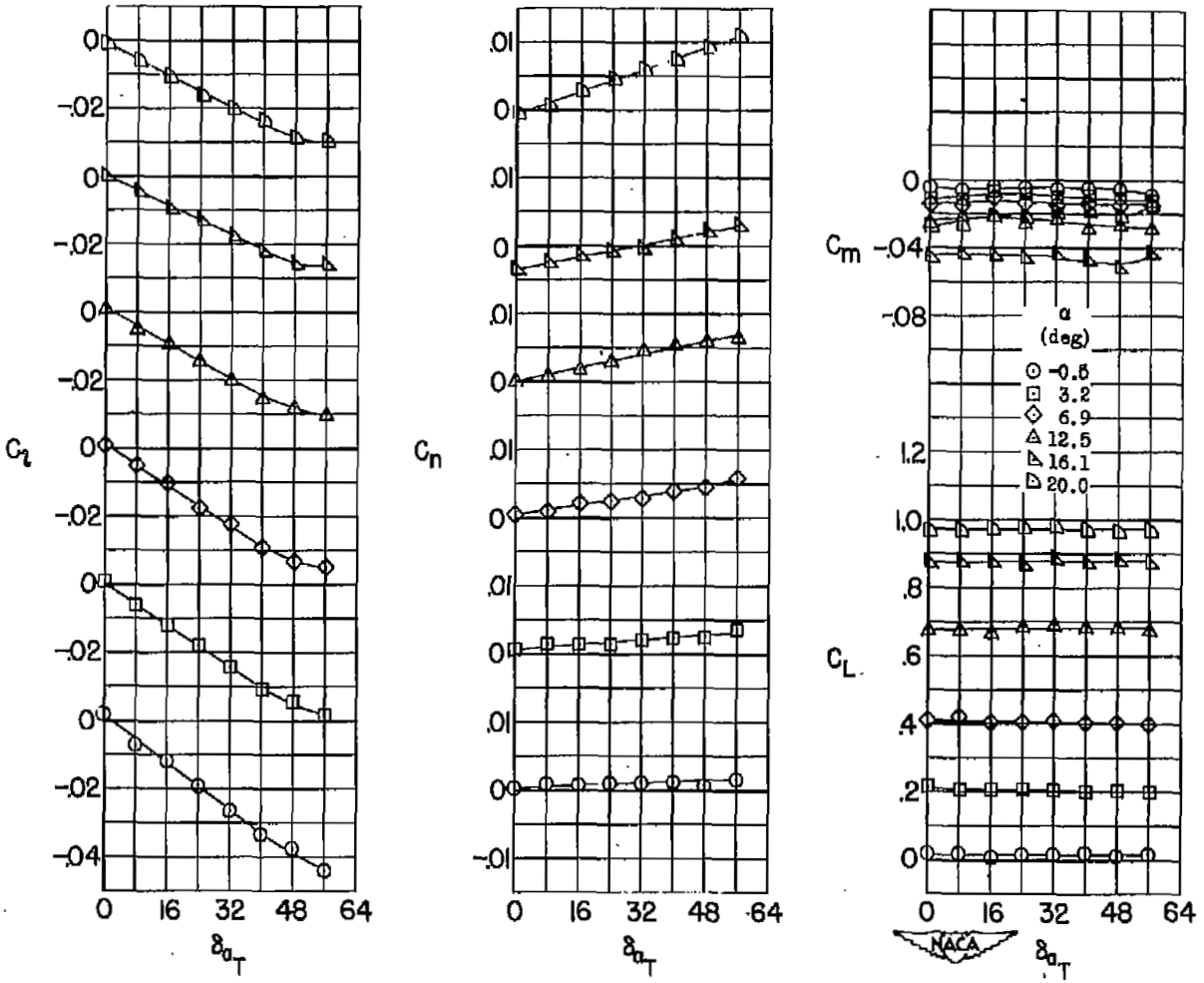

(g) $b_a = 0.45\frac{b}{2}$; $y_{a_o} = 1.00\frac{b}{2}$; $t = 0.25$.

Figure 12.- Continued.

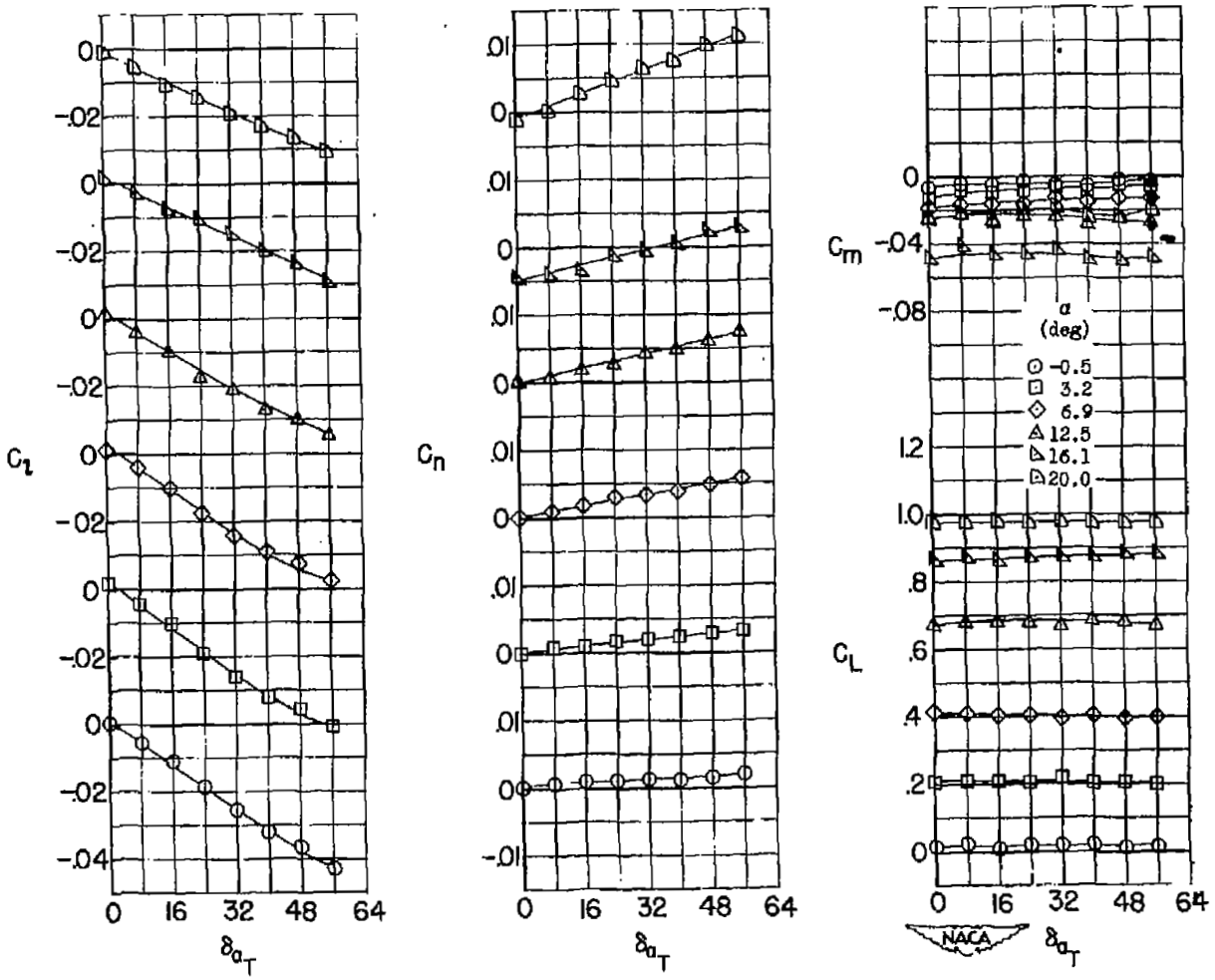

(h) $b_a = 0.45\frac{b}{2}$; $y_{a_o} = 1.00\frac{b}{2}$; $t = 0.50$.

Figure 12.- Continued.

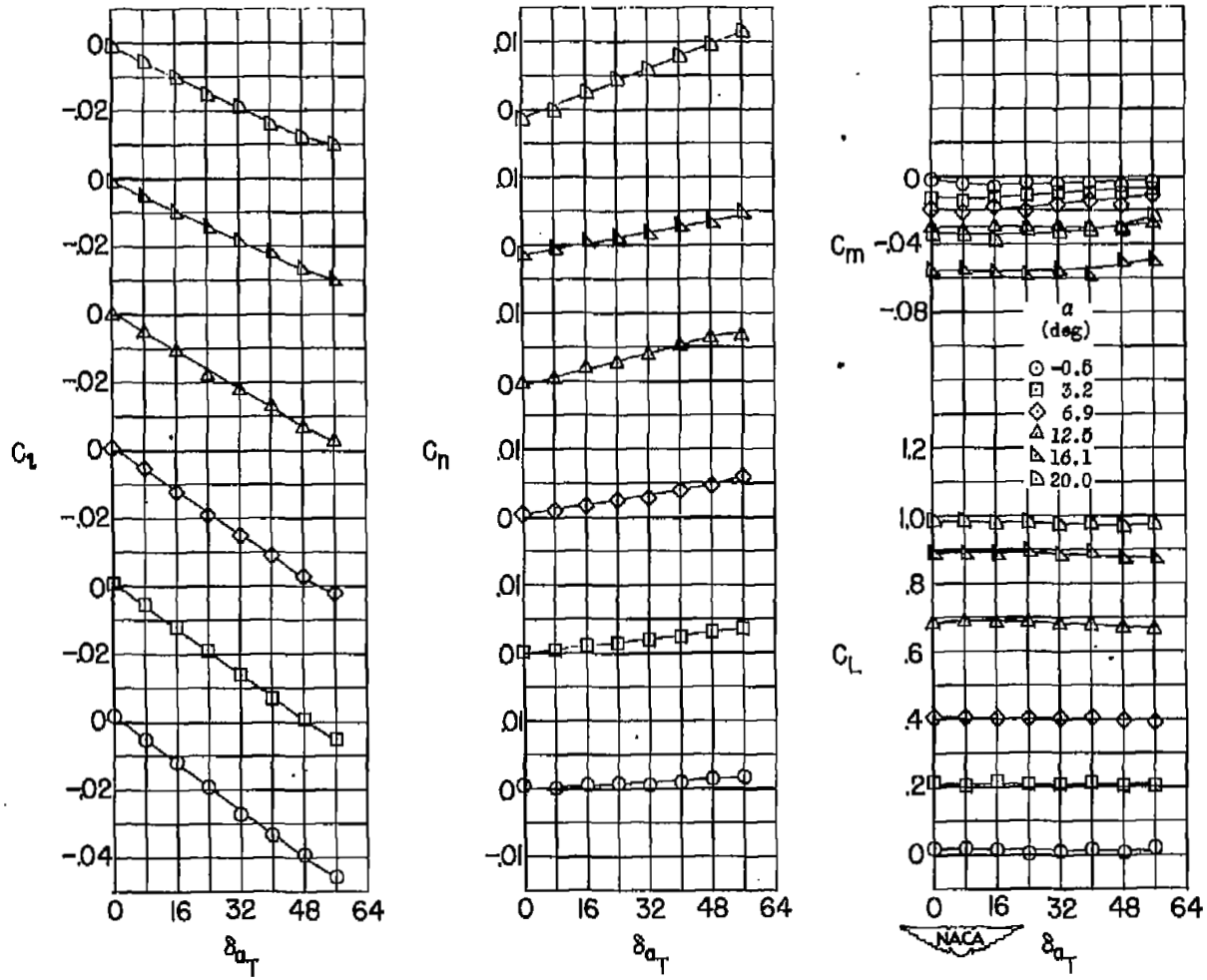

(i) $b_a = 0.45\frac{b}{2}$; $y_{a_o} = 1.00\frac{b}{2}$; $t = 0.75$.

Figure 12.- Concluded.

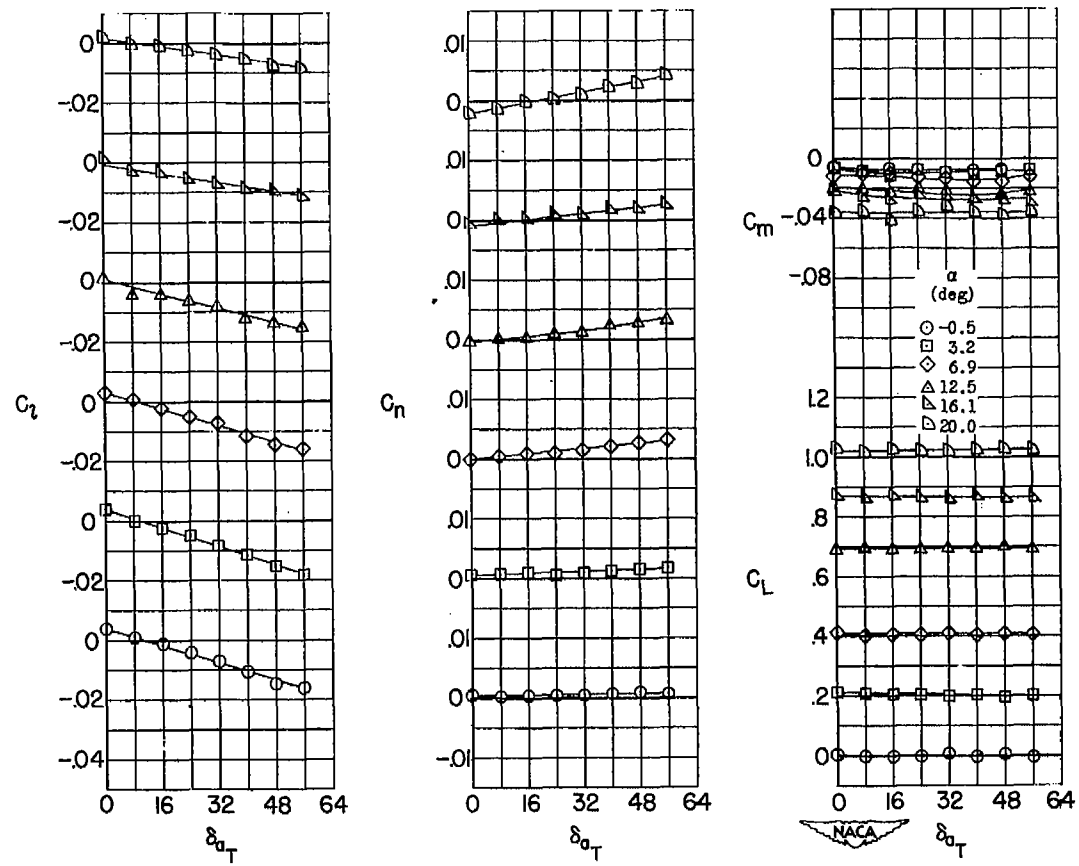

(a) $b_a = 0.225\frac{b}{2}$; $y_{a_o} = 1.00\frac{b}{2}$; $t = 0$.

Figure 13.- Effect of aileron span and trailing-edge thickness on the aerodynamic characteristics of the 47.5° sweptback-wing - fuselage combination with extensible leading-edge flaps. $b_{f_{LE}} = 0.35\frac{b}{2}$; $\delta_{LE} = 150°$; $R = 4.4 \times 10^6$.

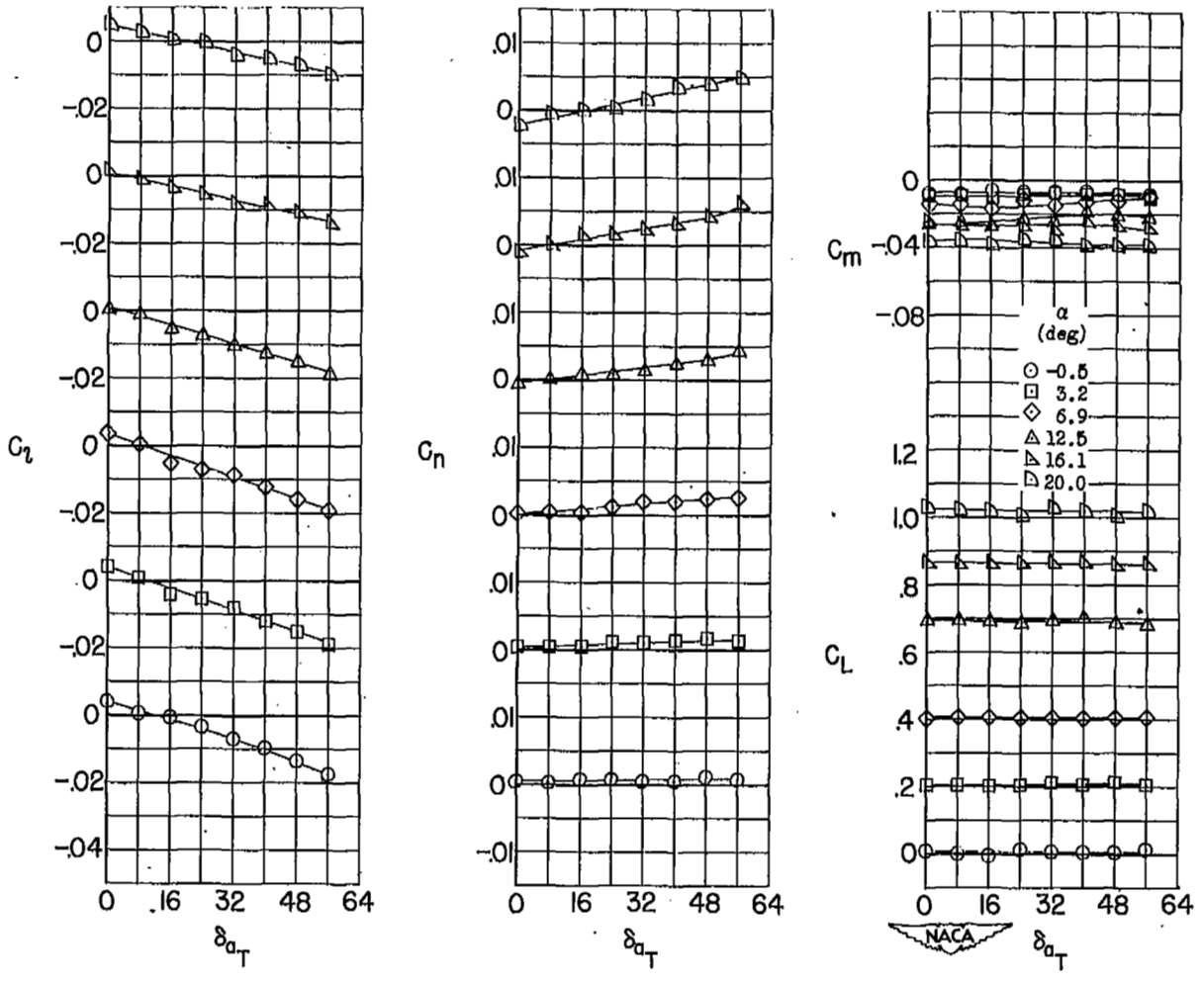

(b) $b_a = 0.225\frac{b}{2}$; $y_{a_o} = 1.00\frac{b}{2}$; $t = 0.50$.

Figure 13.- Continued.

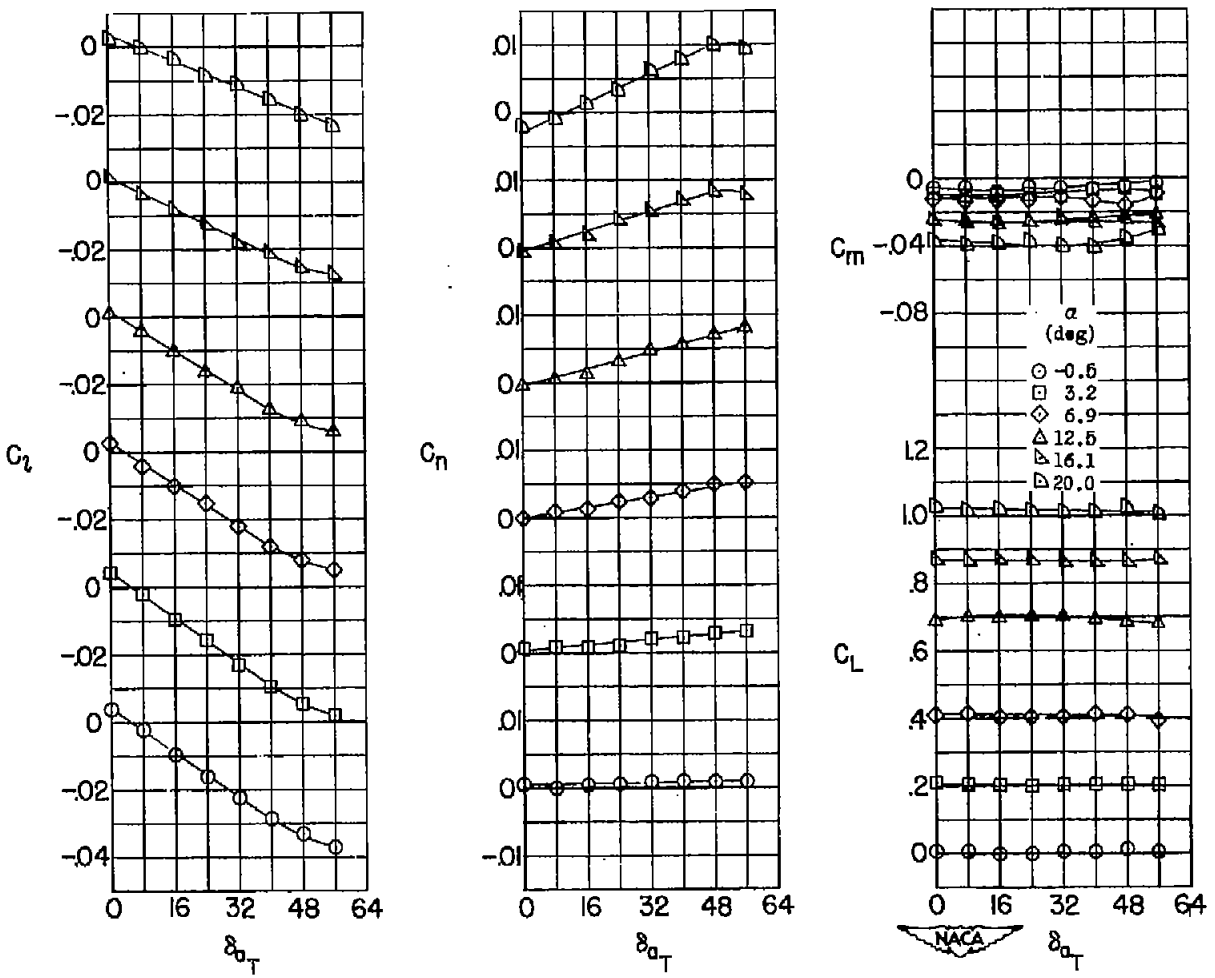

(c) $b_a = 0.45\frac{b}{2}$; $y_{a_o} = 1.00\frac{b}{2}$; t = 0.

Figure 13.- Continued.

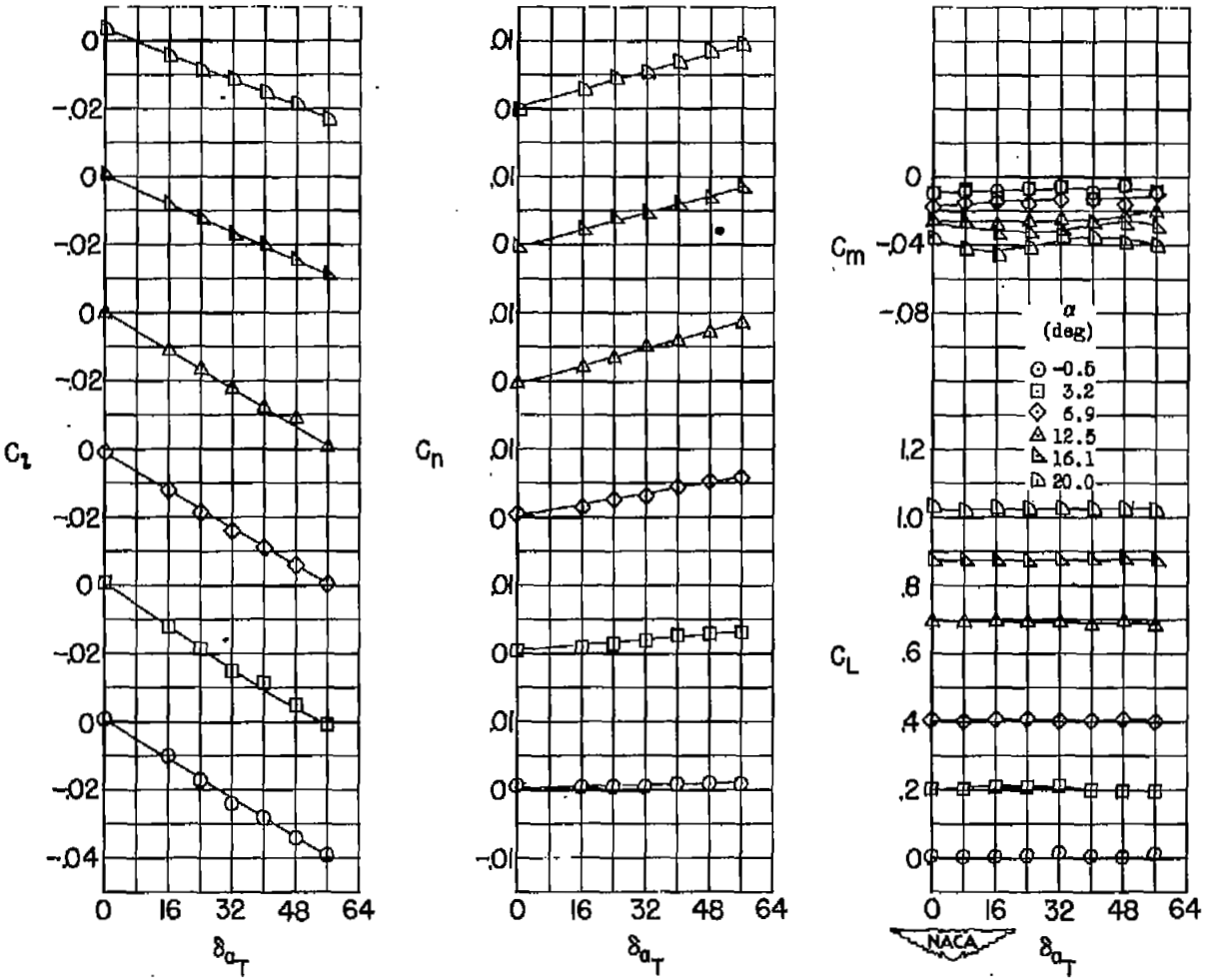

(d) $b_a = 0.45\frac{b}{2}$; $y_{a_o} = 1.00\frac{b}{2}$; $t = 0.50$.

Figure 13.- Concluded.

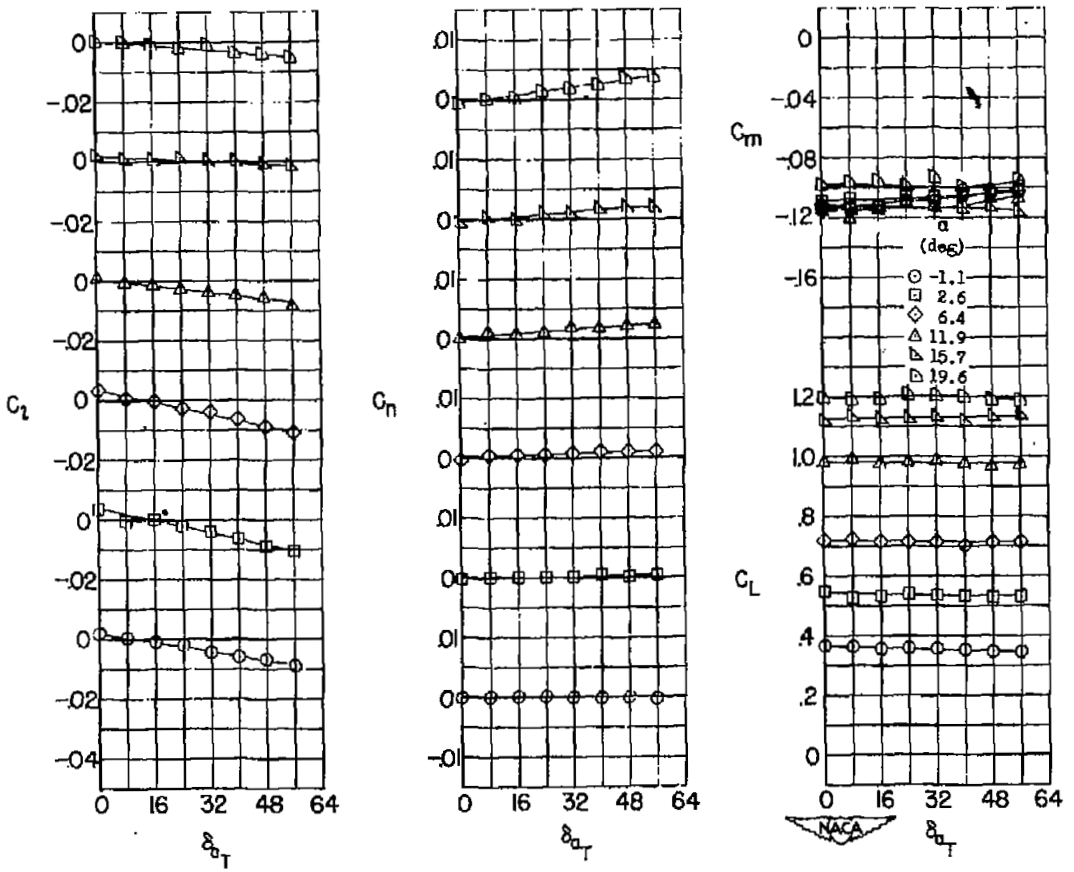

(a) $b_a = 0.225\frac{b}{2}$; $y_{a_o} = 1.00\frac{b}{2}$; $b_{f_{TE}} = 0.655\frac{b}{2}$; $t = 0$.

Figure 14.- Effect of aileron span on the aerodynamic characteristics of the 47.5° sweptback-wing - fuselage combination with extensible leading-edge and plain trailing-edge flaps. $b_{f_{LE}} = 0.35\frac{b}{2}$; $\delta_{LE} = 135°$; $R = 4.4 \times 10^6$.

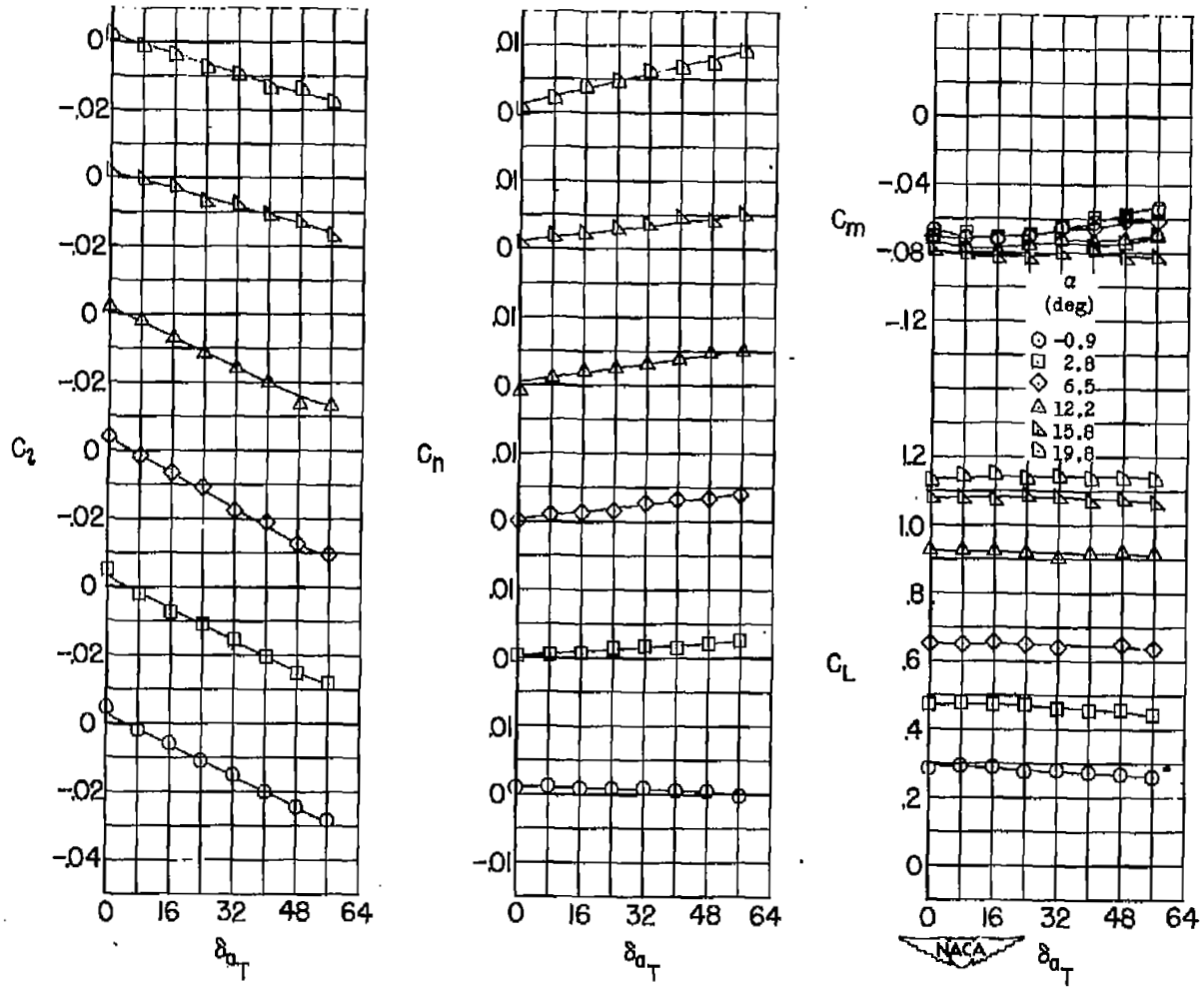

(b) $b_a = 0.45\frac{b}{2}$; $y_{a_o} = 1.00\frac{b}{2}$; $b_{f_{TE}} = 0.43\frac{b}{2}$; t = 0.

Figure 14.- Concluded.

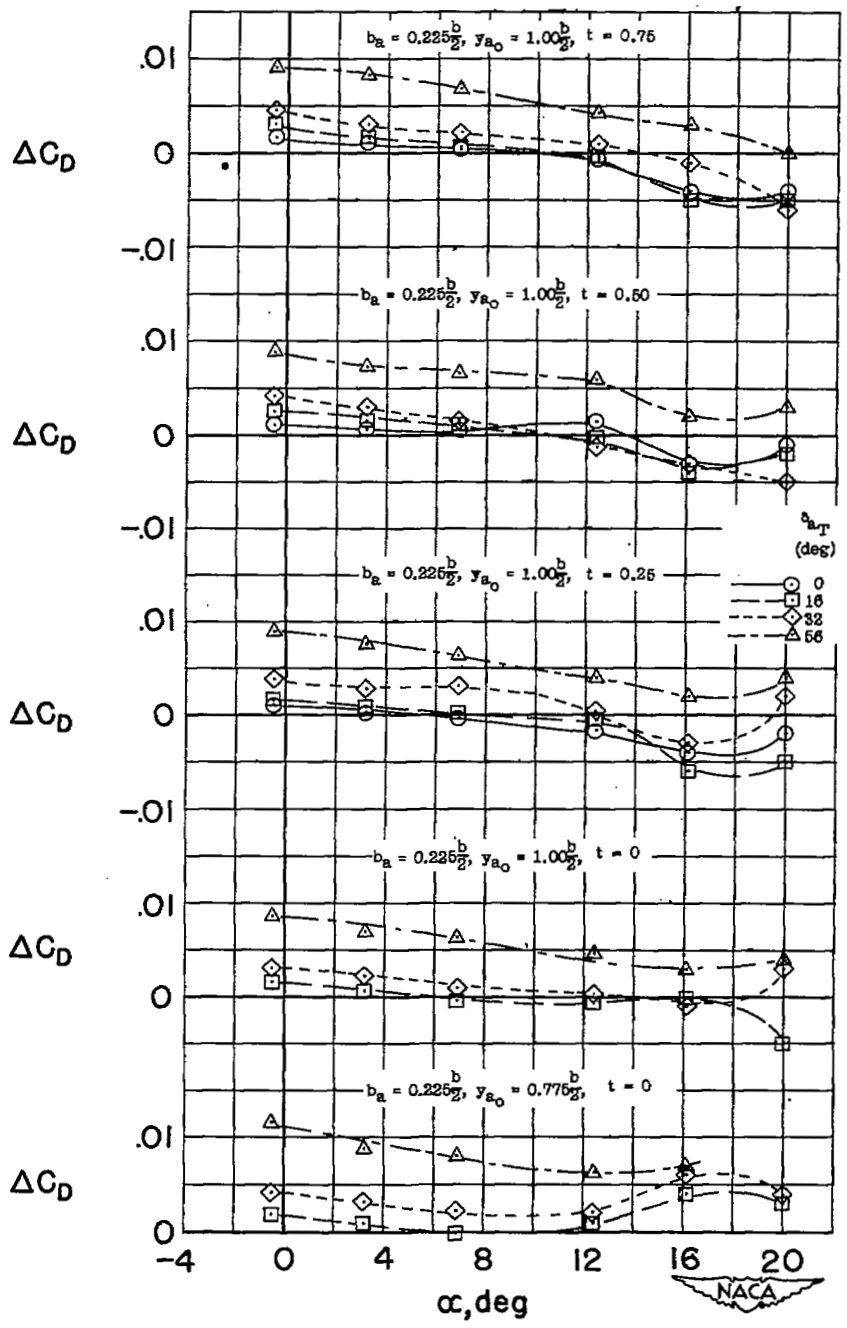

(a) Basic wing.

Figure 15.- Effect of aileron-deflection angle on the drag coefficients of the 47.5° sweptback-wing - fuselage combination for several aileron span and trailing-edge thickness. $R = 4.4 \times 10^6$.

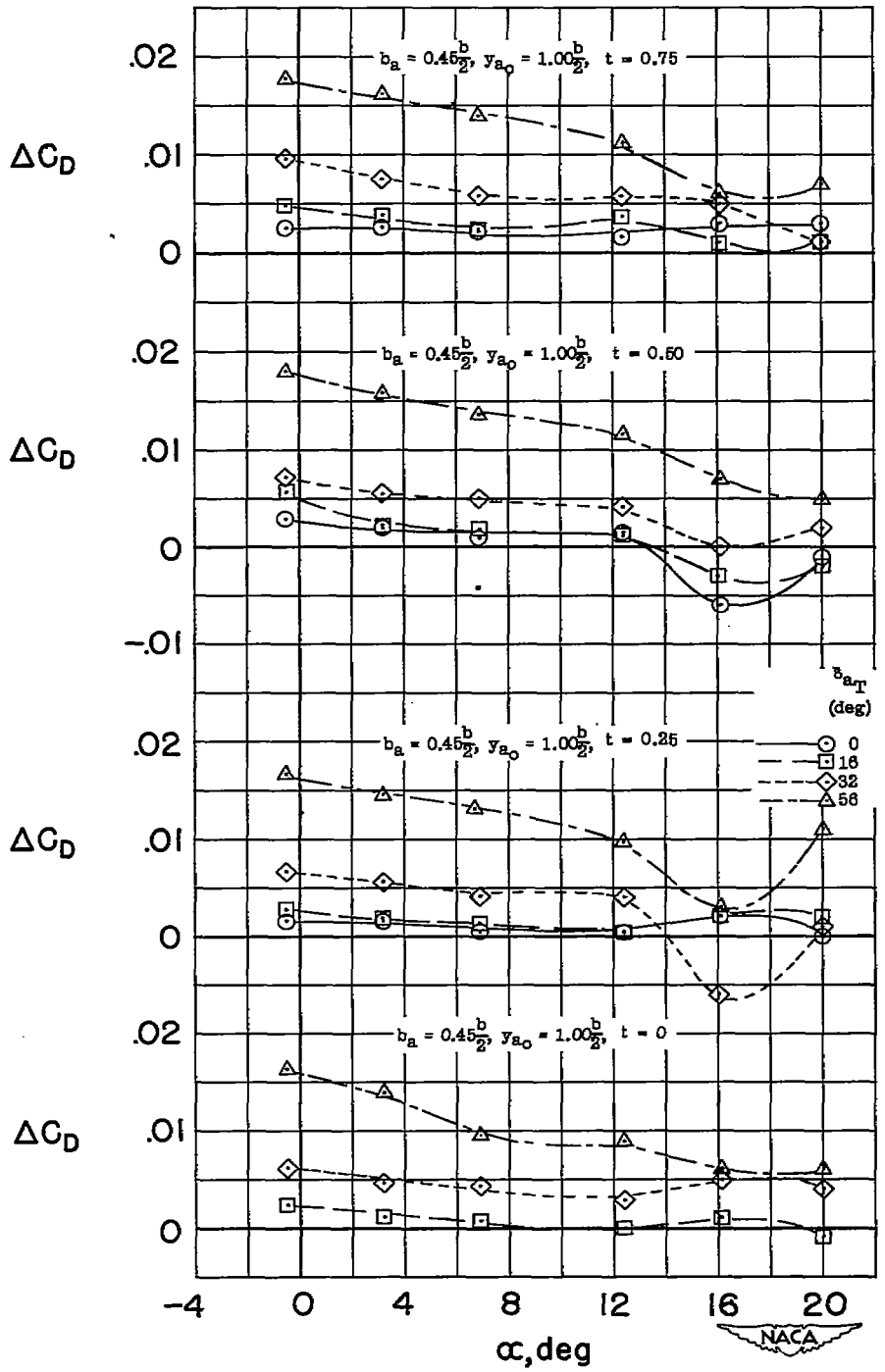

(b) Basic wing.

Figure 15.- Continued.

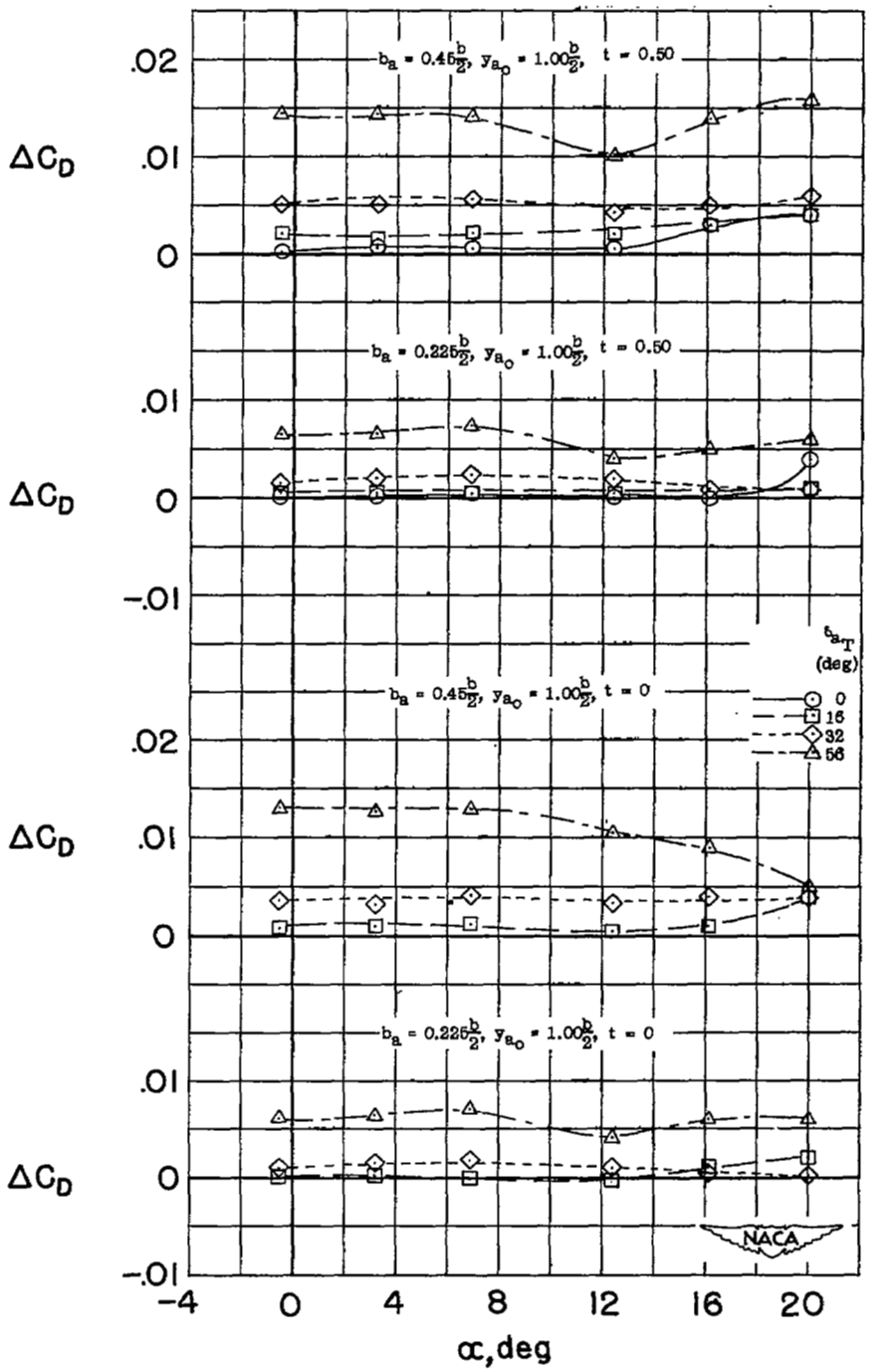

(c) Extensible leading-edge flaps. $b_{f_{LE}} = 0.35\frac{b}{2}$; $\delta_{LE} = 150°$.

Figure 15.- Continued.

[redacted]

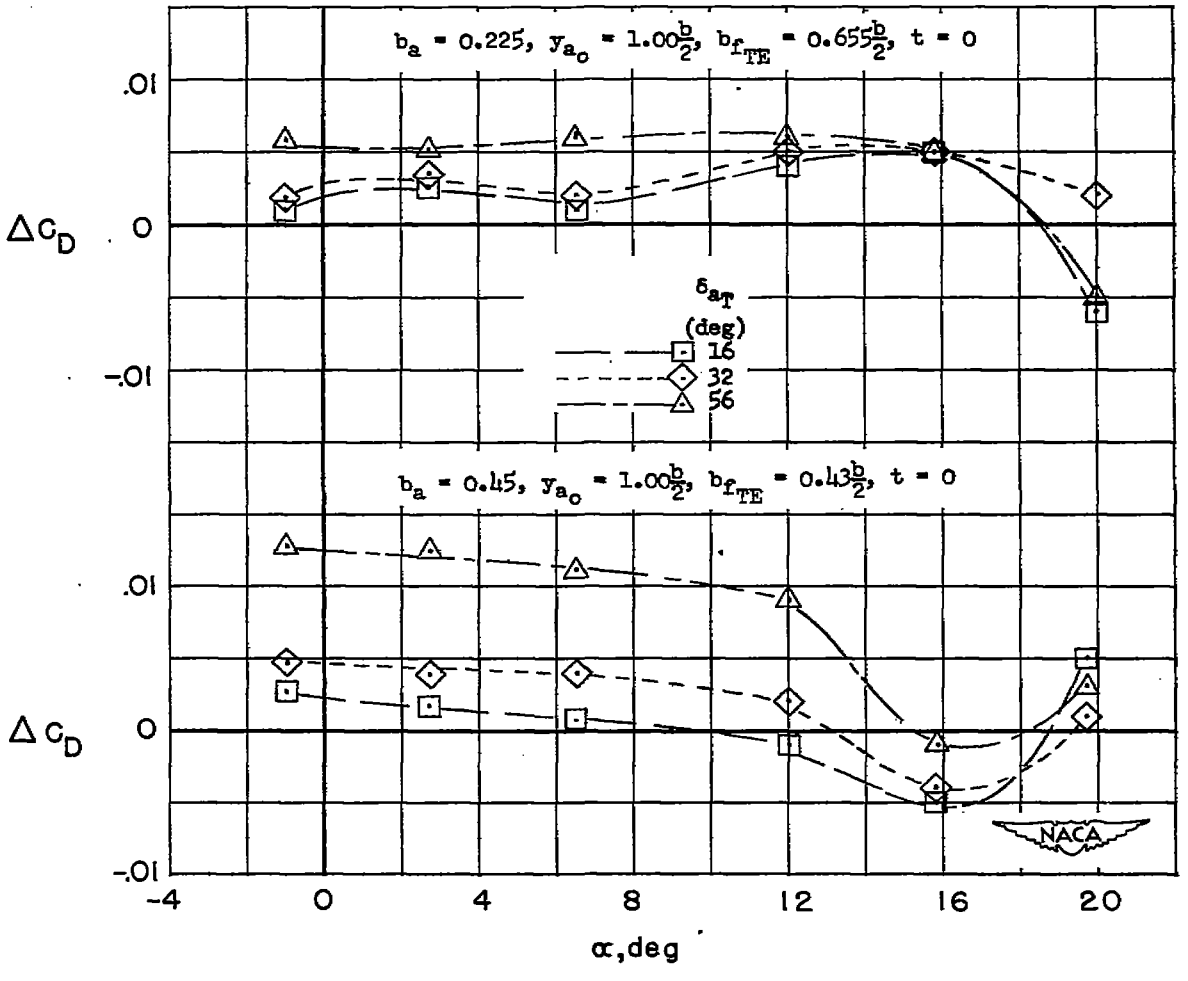

(d) Extensible leading-edge and plain trailing-edge flaps. $b_{f_{LE}} = 0.35\frac{b}{2}$; $\delta_{LE} = 135^{\circ}$.

Figure 15.- Concluded.

[redacted]

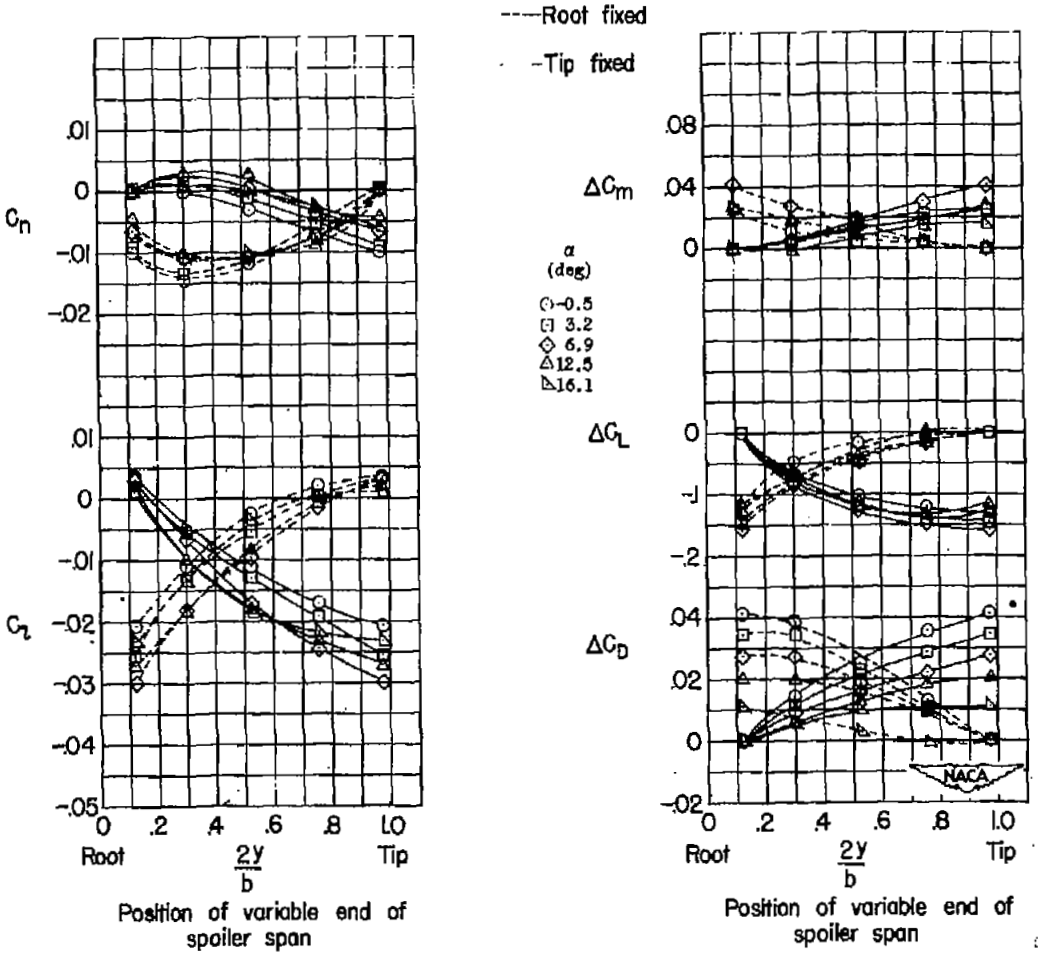

(a) $\delta_s = 0.10c'$.

Figure 16.- Effect of spoiler span and height on the aerodynamic characteristics of the 47.5° sweptback-wing - fuselage combination. $R = 4.4 \times 10^6$.

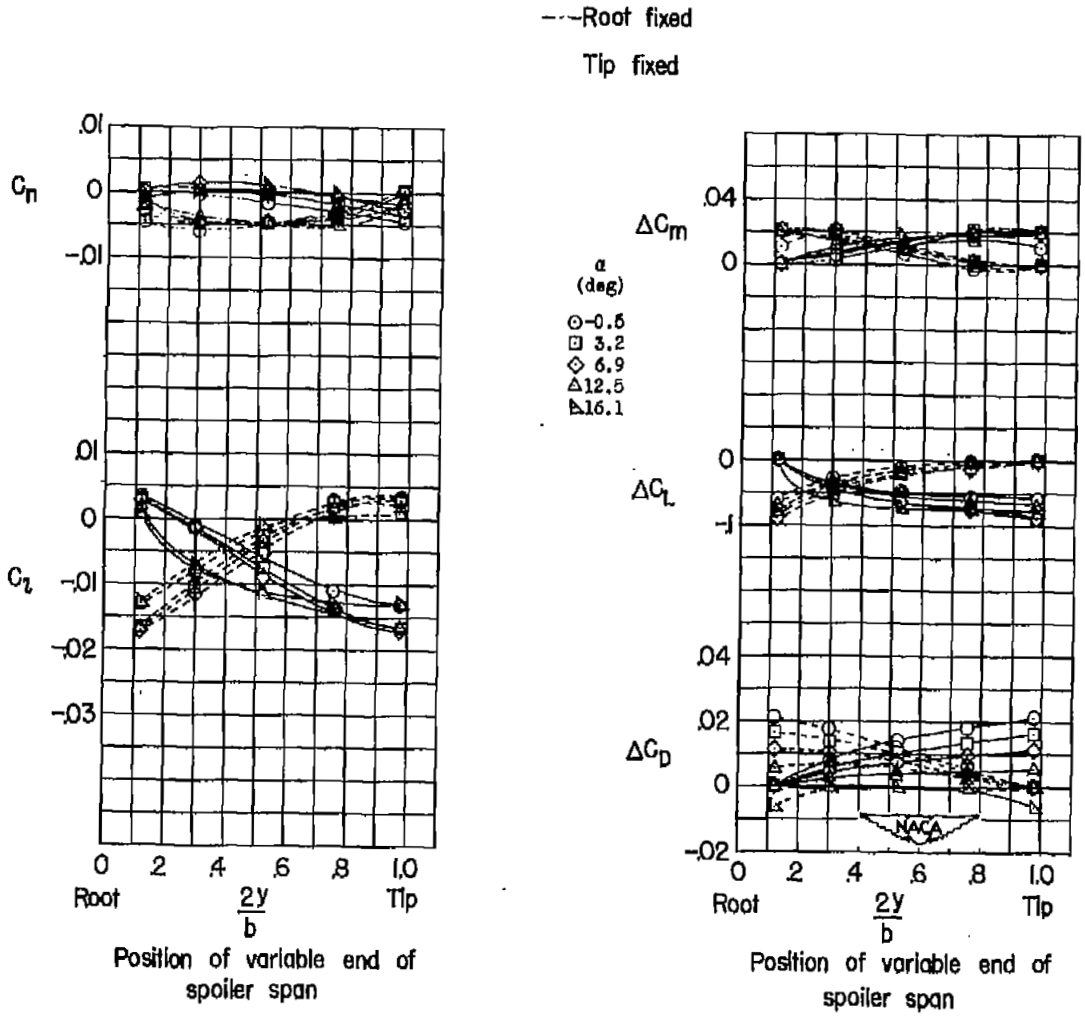

(b) $\delta_s = 0.05c'$.

Figure 16.- Continued.

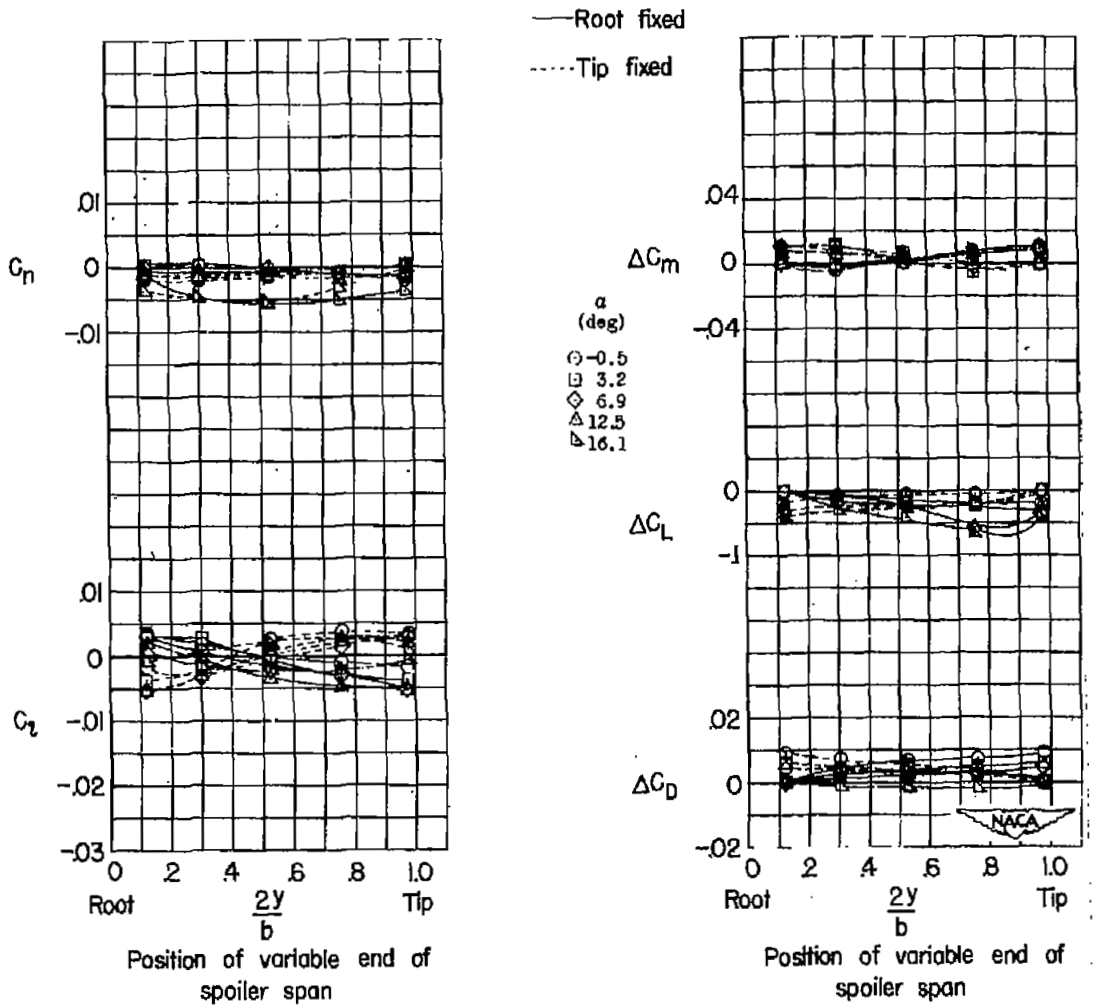

(c) $\delta_s = 0.02c'$.

Figure 16.- Concluded.

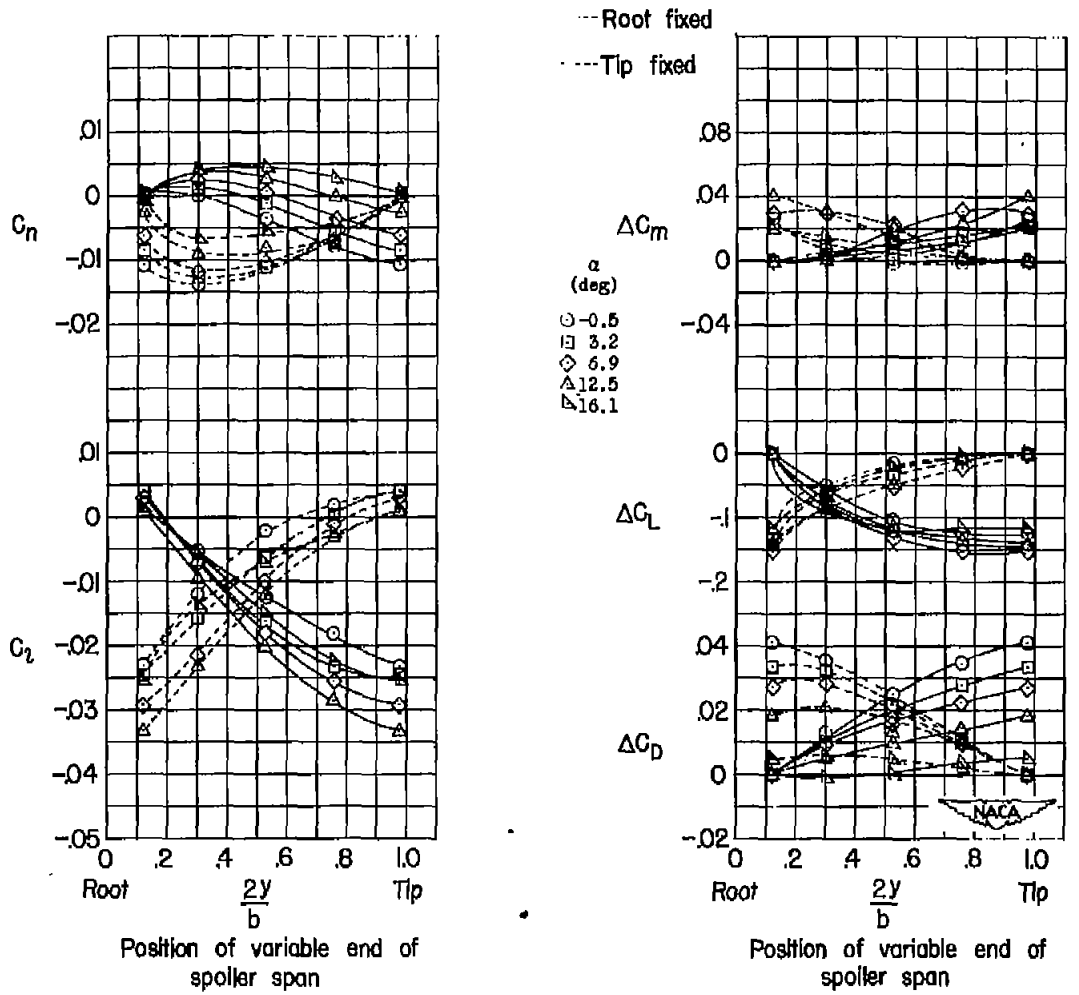

Figure 17.- Effect of spoiler span on the aerodynamic characteristics of the 47.5° sweptback-wing - fuselage combination with extensible leading-edge flaps. $b_{f_{LE}} = 0.35\frac{b}{2}$; $\delta_{LE} = 150°$; $\delta_s = 0.10c'$; $R = 4.4 \times 10^6$.

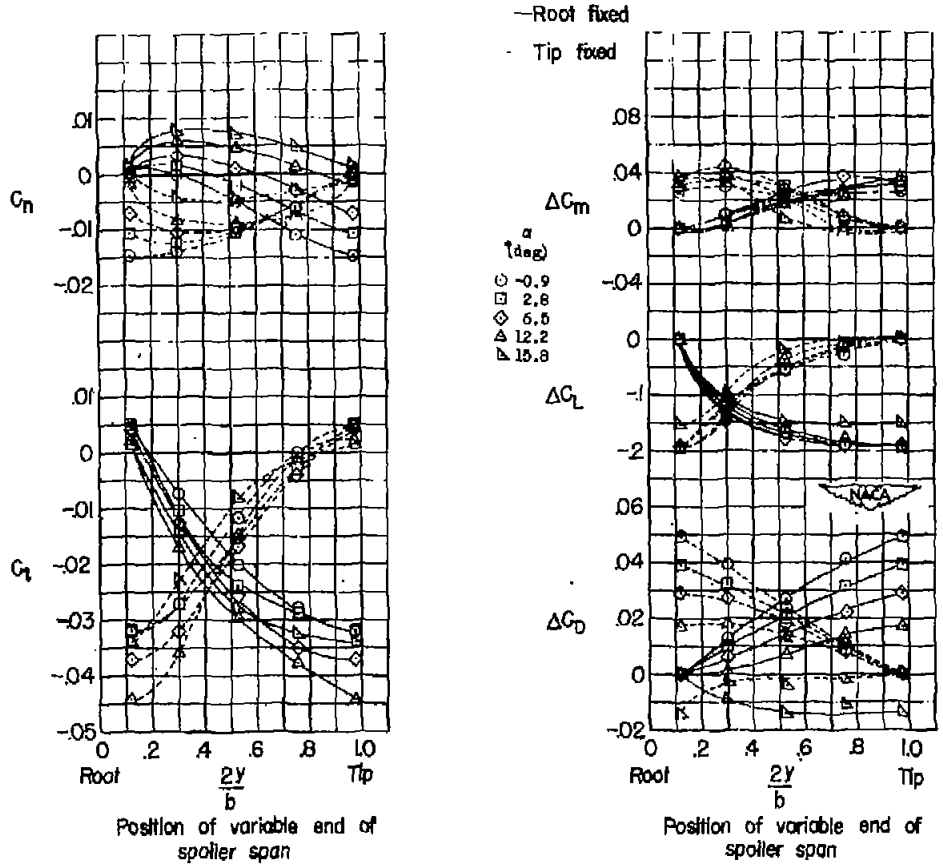

(a) $b_{f_{TE}} = 0.43\frac{b}{2}$; $\delta_s = 0.10c'$.

Figure 18.- Effect of spoiler span and height on the aerodynamic characteristics of the 47.5° sweptback-wing - fuselage combination with extensible leading-edge and plain trailing-edge flaps. $b_{f_{LE}} = 0.35\frac{b}{2}$; $\delta_{LE} = 135°$; $R = 4.4 \times 10^6$.

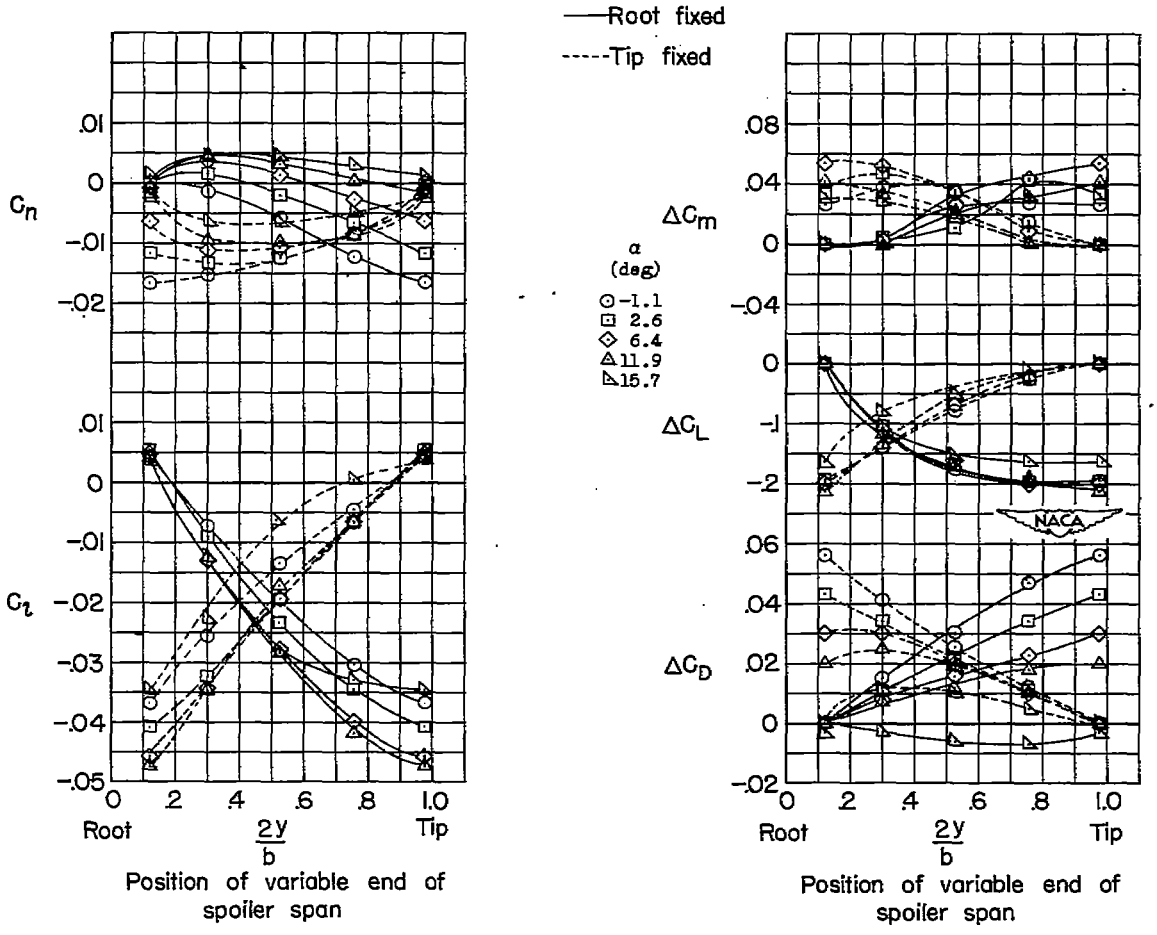

(b) $b_{f_{TE}} = 0.88\frac{b}{2}$; $\delta_s = 0.10c'$.

Figure 18.- Continued.

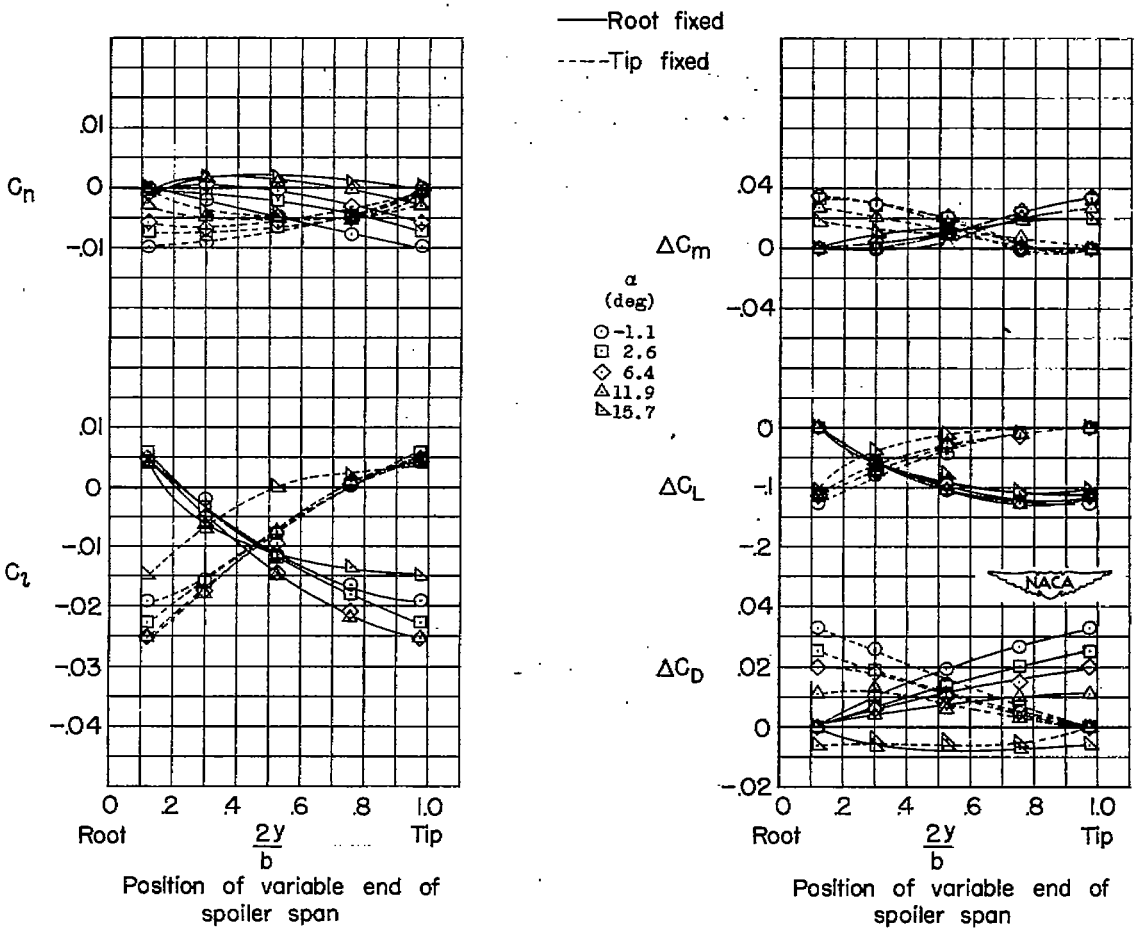

(c) $b_{f_{TE}} = 0.88\frac{b}{2}$; $\delta_s = 0.05c'$.

Figure 18.- Continued.

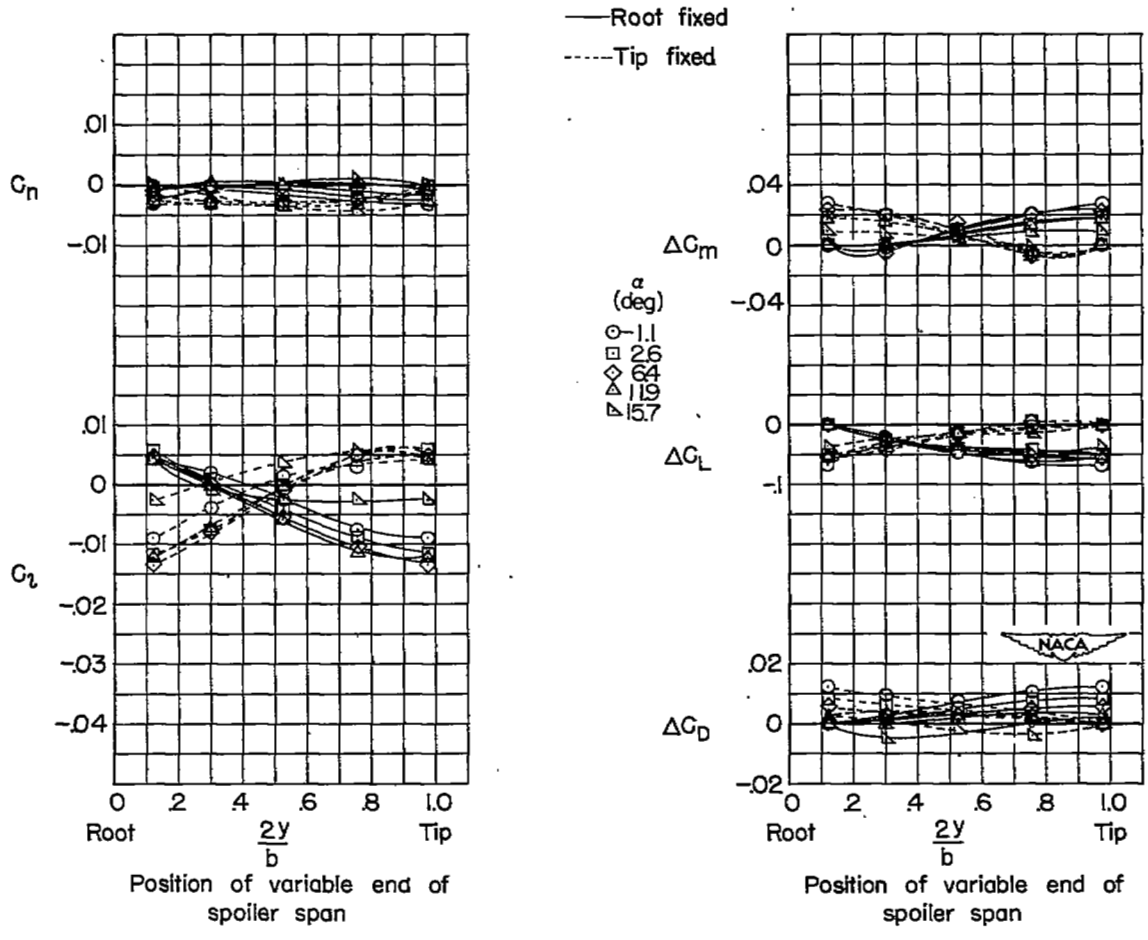

(d) $b_{f_{TE}} = 0.88\frac{b}{2}$; $\delta_s = 0.02c'$.

Figure 18.- Concluded.

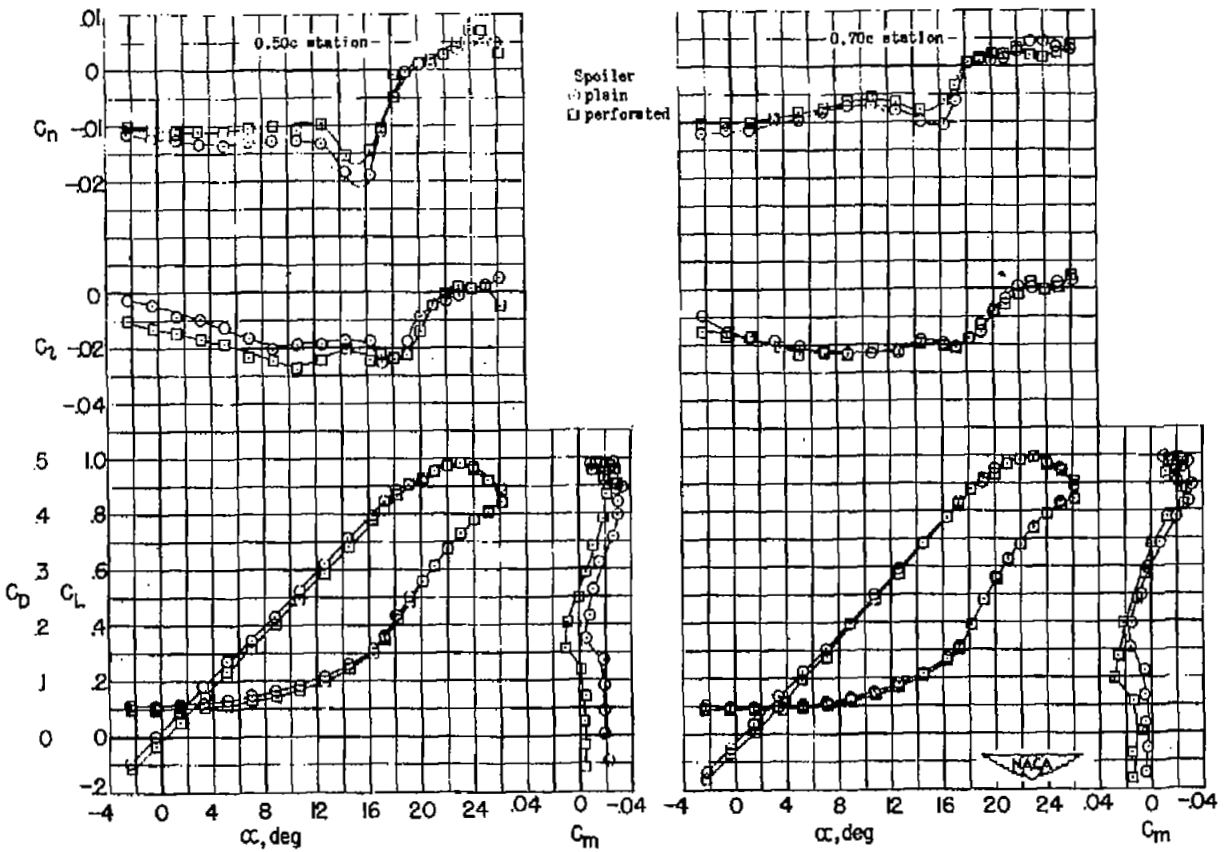

(a) Basic wing.

Figure 19.- Effect of spoiler chord location on the aerodynamic characteristics of the 47.5° sweptback-wing - fuselage combination with plain and perforated spoilers. $b_s = 0.63\frac{b}{2}$; $y_{s_o} = 0.863\frac{b}{2}$; $\delta_s = 0.10c'$; $R = 4.4 \times 10^6$.

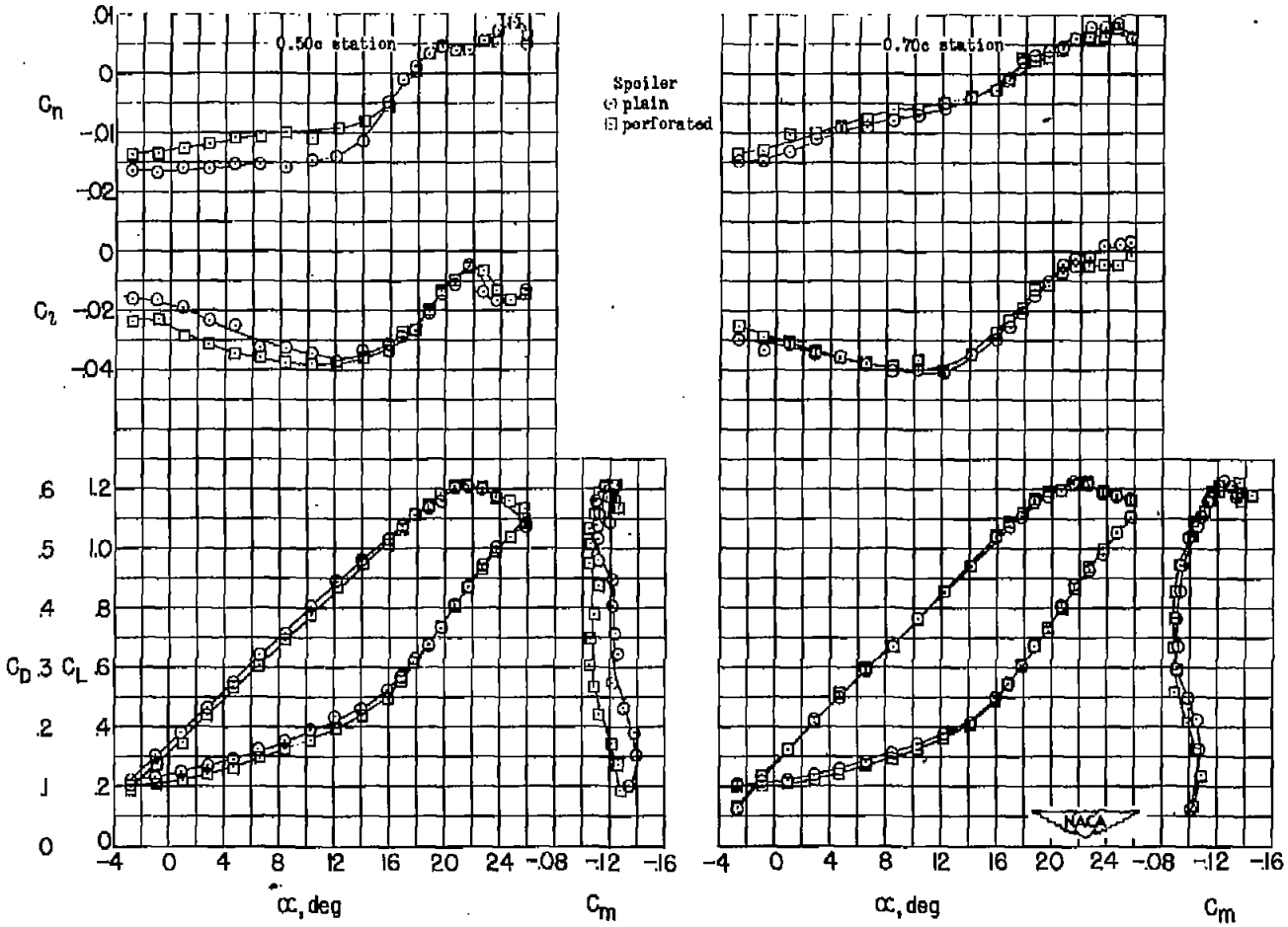

(b) Extensible leading-edge and plain trailing-edge flaps. $b_{f_{LE}} = 0.35\frac{b}{2}$; $\delta_{LE} = 135^{\circ}$; $b_{f_{TE}} = 0.88\frac{b}{2}$.

Figure 19.- Concluded.